# Article (refereed) - postprint

Copeland, Nichola; Cape, J. Neil; Nemitz, Eiko; Heal, Mathew R. 2014.
**Volatile organic compound speciation above and within a Douglas fir forest**.

1    **Volatile organic compound speciation above and within a Douglas Fir forest**

2

3                    Nichola Copeland [1,2], J. Neil Cape [1], Eiko Nemitz [1], Mathew R. Heal [2]

4

5    [1] Centre for Ecology & Hydrology, Bush Estate, Penicuik, EH26 0QB, UK

6    [2] School of Chemistry, University of Edinburgh, West Mains Road, Edinburgh, EH9 3JJ, UK

7

8    Corresponding author:

9    Dr M. R. Heal (address as above)

10    Email: m.heal@ed.ac.uk

11

12

13

14    **Highlights**

15    Concentrations and fluxes measured using PTR-MS with virtual disjunct eddy covariance

16    First non-terpenoid species fluxes and mixing ratios for Douglas fir canopy

17    Above-canopy emissions of monoterpenes comparable to previous studies of *P. menziesii*

18    Fluxes of several non-terpenoid VOCs were significant

19    Acetaldehyde, acetone & MTs elevated near bottom of canopy, MBO & estragole at top

20

21  **Abstract**

22  Mixing ratios and fluxes of volatile organic compounds (VOCs) were measured by PTR-MS

23  (and GC-MS) and virtual disjunct eddy covariance during a three-week field campaign in

24  summer 2009 within and above a Douglas fir (*Pseudotsuga menziesii*) forest in Speulderbos,

25  the Netherlands. Measurements included the first non-terpenoid species fluxes and mixing

26  ratios for Douglas fir canopy. Above-canopy emissions of monoterpenes were comparable to

27  previous studies of *P. menziesii*, with standard emission factors for the first and second halves

28  of the campaign of $0.8 \pm 0.4$ and $0.8 \pm 0.3$ µg $g_{dw}^{-1}$ $h^{-1}$, and temperature coefficients of $0.19 \pm$

29  $0.06$ and $0.08 \pm 0.05$ $^{\circ}C^{-1}$, respectively. Isoprene standard emission factors for the two halves

30  of the campaign were $0.09 \pm 0.12$ and $0.16 \pm 0.18$ µg $g_{dw}^{-1}$ $h^{-1}$. Fluxes of several non-

31  terpenoid VOCs were significant, with maximum fluxes greater than has been measured for

32  other coniferous species. α-Pinene was the dominant monoterpene within and above the

33  canopy. Within canopy mixing ratios of individual species were generally greatest in early

34  evening consistent with reduced vertical mixing and continued temperature-dependent

35  emissions. Acetaldehyde, acetone and monoterpenes had elevated mixing ratios toward the

36  bottom of the canopy (5-10 m) with assumed contribution from the large quantities of forest-

37  floor leaf litter. MBO (2-methyl-3-buten-2-ol) and estragole had peak mixing ratios at the top

38  of the canopy and are known to have coniferous sources. MVK + MACR (methyl vinyl

39  ketone and methacrolein)  also had highest mixing ratios at the top of the canopy consistent

40  with formation from in-canopy oxidation of isoprene. The work highlights the importance of

41  quantifying a wider variety of VOCs from biogenic sources than isoprene and monoterpenes.

42

43  Key words: BVOC, PTR-MS, vDEC, monoterpene, pinene, isoprene

## 1 Introduction

Emissions of volatile organic compounds (VOC) from vegetation are estimated as about 10 times greater globally than VOC emissions from anthropogenic sources (Guenther et al., 1995; Steiner and Goldstein, 2007). The dominant BVOC is isoprene (Guenther et al., 2006), estimated to contribute 44% of global BVOC emissions, with monoterpenes contributing 11%, and other VOCs comprising the remainder. The high atmospheric reactivity of many BVOC means such emissions have important regional impacts on atmospheric oxidising capacity, and on tropospheric ozone and secondary organic aerosol formation.

Coniferous forests are normally associated with monoterpene emissions and low (or zero) isoprene emissions (Geron et al., 2000; Karl et al., 2009). Douglas fir is reported to be within the top 10 monoterpene-emitting tree species in the USA (Geron et al., 2000) but previous studies on Douglas fir have investigated emissions at the leaf and branch scale. Arey et al. (1995) measured a standardised monoterpene emission rate (at 30 °C and 1000 μmol m$^{-2}$ s$^{-1}$) of 1.1 μg g$_{dw}^{-1}$ h$^{-1}$ for bigcone Douglas fir (*Pseudotsuga macrocarpa*), with α-pinene and limonene as major components, and β-pinene and 3-carene also detected. An emission rate of 0.44 μg g$_{dw}^{-1}$ h$^{-1}$ was reported for coastal Douglas fir (*Pseudotsuga menziesii*) (Pressley et al., 2004). The highest reported standardised monoterpene emission rate is 2.60 μg g$_{dw}^{-1}$ h$^{-1}$ from *Pseudotsuga menziesii* (Drewitt et al., 1998). An isoprene emission rate of 1.72 μg g$_{dw}^{-1}$ h$^{-1}$ was also reported. A study which investigated a wider range of VOC emissions from saplings also detected sesquiterpenes, oxygenated terpene products (including 2-methyl-3-buten-2-ol (MBO)), methyl salicylate and a homoterpene (C$_{11}$H$_{18}$) (Joó et al., 2011).

68  Quantification of VOC emissions from Douglas fir warrants further research due to paucity of

69  data at canopy scale and for non-terpenoid compounds, and the variability in previously

70  reported standard emissions. In this work, fluxes and mixing ratios of VOCs were measured

71  above and within a Douglas fir canopy at Speulderbos, the Netherlands. A previous study at

72  this site measured forest floor and above-canopy mixing ratios of α-pinene, β-pinene, 3-

73  carene and limonene (Dorsey et al., 2004). Monoterpene mixing ratios above the forest floor

74  were greater than those measured above-canopy, which was attributed to leaf litter emissions,

75  and were also greatest at night because of the lower atmospheric mixing. These findings

76  broadly corroborated those of an earlier study (Peters et al., 1994). However, neither of these

77  studies measured fluxes or other VOC species.

78

79  **2 Methods**

80

81  **2.1 Sampling site**

82  Measurements were made from 15 June to 10 July 2009 at an established site in Speulderbos

83  forest near Garderen, Netherlands (52º 15′ N, 5º 41′ E, 50 m asl, Supplementary information

84  Figure S1), operated by RIVM (Rijksinstituut voor Volksgezondheid en Milieu). The forest

85  comprises a dense monoculture of mature Douglas fir (*Pseudotsuga menziesii*, ~2.3 ha, Figure

86  S2), planted in 1960, within a larger forested area (50 km$^2$). The soil is an orthic

87  podzol/holtpodzol with loamy sand texture. The maximum canopy height was ~32 m. Due to

88  the high planting density there was almost no tree foliage below 8 m and little light

89  penetration to the forest floor.

90

91  The nearest settlements to the site are Garderen (2.5 km SE, population ~2,000), Putten (5.7

92  km WNW, population ~23,000) and Ermelo (6.6 km NW, population ~26,000), while the

93  nearest major city is Apeldoorn (19 km ESE, population ~156,000). There was very little

94  traffic on surrounding roads.

95

96  Flux footprints for the sampling location were predicted with a simple parameterisation model

97  (Kljun et al., 2004) using minimum, maximum and mean $u*$ values (Figure S3). The largest

98  distance which encompassed 80% of the flux contribution at the monitoring site across the

99  range of friction velocities encountered during the campaign was 660 m. This distance was

100  within a uniform area of forest for all wind directions (Figure S4).

101

102  **2.2 PTR-MS set-up**

103  BVOC mixing ratios and fluxes above the forest canopy were measured using proton transfer

104  reaction mass spectrometry (PTR-MS) (Blake et al., 2009) coupled with virtual disjunct eddy

105  covariance (vDEC) (Karl et al., 2002; Rinne et al., 2001). The PTR-MS instrument (Ionicon

106  Analytik, Innsbruck, Austria) was fitted with an extra turbopump connected to the detection

107  chamber, and Teflon instead of Viton rings in the drift tube (Copeland et al., 2012; Misztal et

108  al., 2010). Pfeiffer turbopumps replaced the Varian equivalents. Drift tube conditions were

109  held constant throughout (pressure 1.7 mbar, temperature 45 °C, voltage 478 V) to maintain

110  an $E/N$ ratio of ~130 Td (1 Td = $10^{-17}$ V cm$^2$).

111

112  The sampling inlet and 20 Hz sonic anemometer (WindmasterPro, Gill Instruments) were

113  positioned above the canopy at the top of a 45 m tower. Air was sampled at 23.5 L min$^{-1}$

114  through a 50 m PTFE inlet line (1/4″ OD, 3/16″ ID) with a T-piece for sub-sampling into the

115  PTR-MS inlet at a rate of 250 mL min$^{-1}$. Condensation of water vapour in the inlet line was

116  prevented by wrapping with self-regulating heating tape (Omega, UK type SRF3-2C). Data

117  were logged using a program written in LabVIEW (Version 8.5, National Instruments).

118

**2.3 Determination of VOC mixing ratios and fluxes**

119

The PTR-MS signal was calibrated explicitly for several VOCs using a mixed-gas calibration

120

cylinder (Apel-Riemer Environmental Inc., USA) containing 1 ppmv each of formaldehyde,

121

methanol, acetonitrile, acetone, acetaldehyde, isoprene and 0.18 ppmv d-limonene. The

122

calibration gas was diluted with VOC-scrubbed air to produce 6 samples with concentrations

123

of 0.5, 1.0, 10, 20, 30 and 50% of the pure calibration gas standard. A relative transmission

124

curve was constructed to determine empirical calibration coefficients for other VOCs under

125

study not present in the standard (Taipale et al., 2008). Calibrations were carried out in the lab

126

before commencement of the field campaign, and on 8 July during the campaign. Limits of

127

detection (LOD) were calculated as twice the standard deviation of the background ion counts

128

for a particular $m/z$ divided by sensitivity (ncps ppbv$^{-1}$) (Karl et al., 2003). Detailed

129

information on cross-check of the PTR-MS calibration is given in the supplementary material

130

of Misztal et al. (2011).

131

132

For the first 10 days of measurements (18-28 June) the PTR-MS operated in multiple ion

133

detection (MID) mode for two 25 min periods per hour. During these periods only the

134

targeted VOC ions listed in Table 1 were measured (0.5 s dwell times), in addition to the

135

primary ion $H_3O^+$, and water cluster $(H_2O)H_3O^+$ (0.2 s dwell times). This gave a sampling

136

cycle time over the 14 target $m/z$ values in Table 1 of 6.4 s, with each of the organic target

137

masses sampled for 0.5 s in each cycle. Sensitivities and LODs for target ions are given in

138

Table 1. The remaining 10 min per hour was used for full mass scans in the range 21–206

139

amu at a dwell time of 1 s per amu. For one 5 min period, ambient air was scanned to allow

140

information about full VOC composition to be acquired. For a further 5 min per hour, 'zero

141

air' was scanned to determine instrument background. Zero air was achieved by sampling

142

143 ambient air through a zero-air generator comprising a glass tube packed with platinum wool

144 and a 50:50 mixture of platinum mesh and activated charcoal heated to 200 °C. The

145 background spectrum was subtracted in subsequent data processing.

146

147 As the PTR-MS was run in MID mode, fewer data points were generated than required for

148 direct eddy covariance due to the non-continuous manner in which the quadrupole mass

149 analyser measures each $m/z$. The set-up resulted in 30,000 wind speed measurements and up

150 to 203 VOC measurements in each 25 min sampling period. The lag time between PTR-MS

151 and wind speed data due to residence time in the sampling inlet line and disjunction between

152 sonic and PTR-MS data was determined by finding the maximum in cross-correlation

153 between vertical wind speed and VOC mixing ratio as a function of lag time (with 15 s

154 window). A program written in LabVIEW was used to determine lag times separately for

155 each compound within each 25 min flux sampling period. Mean lag times were in the range

156 6.5 to 7.1 s. This includes an estimated transition time of 2.3 s between the sampling point

157 and analyser input; the remainder resulted from delays in the data-handling software.

158

159 Quality control criteria were applied to filter data for periods of low friction velocity ($u^*$ <0.15

160 m s$^{-1}$), non-stationarity, large spikes in vertical wind speed or VOC concentration, and where

161 <10,000 data points (5.5 % of all data) were acquired in a 25 min sampling period. Most

162 discarded data occurred during night when turbulence was low (48.3% of all data points).

163 High-frequency flux losses due to relatively slow disjunct VOC sampling frequency (2 Hz,

164 compared to 20 Hz sonic data capture) were estimated using empirical ogive analysis

165 (Ammann et al., 2006) for each 25 min period and flux values corrected accordingly.

166 Standard rotations of the coordinate frame were applied to correct for sonic anemometer tilt

167 for each 25 min period separately.

168

**2.4 In-canopy measurements**

From 30 June to 7 July in-canopy mixing ratios were also measured. A pulley system allowed

continuous movement of the PTR-MS inlet between heights of 4 and 32 m. During this

period, above-canopy measurements were taken during the first half of every hour (hh:05 to

hh:30) and in-canopy measurements were taken in the latter half of every hour (hh:35 to

hh:00). Full mass scans of ambient air and zero air were taken for 5 min intervals at hh:00 and

hh:30 respectively. PAR and temperature were also measured from the gradient system.

**2.5 Chromatographic analysis of ambient air samples**

Ambient air samples were collected above the canopy on 6 July 2009 for subsequent GC-MS

analysis. Samples were also taken at heights of 32, 18 and 4 m three times during the day on 1

and 6 July 2009. The collection of these samples was for spot inter-comparison against the

continuous PTR-MS data, and to provide an indication of speciation between α-pinene and β-

pinene, which the PTR-MS cannot distinguish. Given the limited dataset from these

measurements, the detail of the methods and results are presented in the Supplementary

Information, with key observations highlighted here.

**3 Results**

**3.1 Above canopy fluxes**

The full time series of above-canopy VOC fluxes along with $u*$ and sensible heat flux are

shown in Figure S5. Two periods of missing data 25-26 June and 3 July were due to problems

with a data communication cable and the sampling pump, respectively. Most missing data at

night were due to exclusion of low $u*$ values. The winch set-up commenced 29 June at 20:00,

193   after which above-canopy data were hourly rather than half-hourly. Because of the difference

194   in measurement frequency, data from the two halves of the campaign were treated separately.

195   Diurnal profiles of VOC fluxes for the first half are shown in Figure 1. Since raw flux data

196   were relatively noisy, median values were calculated for each half-hourly time step and the 3-

197   hour running mean plotted e.g. the data point plotted for 12:00 is the mean of median values

198   from 10:30 to 13:30.

199

200   Positive daytime fluxes were discernible for acetaldehyde, acetone and monoterpenes, with

201   near-zero or depositional fluxes at night following the sharp decrease in sensible heat flux.

202   (Note that the term 'zero' here should be interpreted in the context of the variability in values

203   encapsulated by the grey shading of Figure 1.) Diurnal trends in methanol and isoprene fluxes

204   were similar, with minima ($\sim$ $-0.8$ and $\sim$ $-0.15$ mg m$^{-2}$ h$^{-1}$, respectively) during the day and

205   maxima ($\sim$0.5 and $\sim$0.2 mg m$^{-2}$ h$^{-1}$, respectively) in the evening or at night. This was

206   particularly pronounced for isoprene, which had a sharp increase in emission to its maximum

207   between 12:00 and 18:00, coinciding with maximum PAR, before decreasing rapidly to zero

208   towards sunset. The diurnal pattern of isoprene oxidation products MVK + MACR fluctuated

209   throughout the day with small positive fluxes in the morning and early evening, when

210   isoprene emissions declined but isoprene photo-oxidation continued.

211

212   Fluxes of hexanals and MBO were near-zero except for some positive fluxes between 18:00

213   and 00:00. Conversely, TMA, *p*-cymene and estragole had negative fluxes in the evening,

214   with TMA and *p*-cymene fluxes around zero for the remainder of the day and estragole

215   having positive fluxes overnight. However, the majority of these fluxes were below LOD.

216

217    There was a discrepancy in monoterpene fluxes determined from *m/z* 81 and *m/z* 137 ions

218    with the latter yielding greater values. The inconsistency may be due to differences in

219    fragmentation patterns between monoterpenes, as has been observed in other studies (Rinne et

220    al., 2007). Measurements for MT137 were also below LOD so determinations at MT81 are

221    likely more reliable.

222

223    Diurnal profiles were noisier for the second half of the campaign because of the less frequent

224    sampling (Figure S6). Absolute fluxes tended to be greater during the second half, as were

225    temperatures. Daily patterns showed some similarities to those in the first half but were less

226    distinct.

227

228    **3.2 Above-canopy mixing ratios**

229    The full time series of above-canopy mixing ratios and temperature are shown in Figure S7.

230    Average diurnal profiles of VOC mixing ratios for the first half of the campaign are shown in

231    Figure 2. All compounds, except *p*-cymene, had similar daily patterns of minima around

232    midday and maxima at night. Amplitudes of diurnal cycle were small for most compounds,

233    with those for methanol, acetaldehyde and acetone being most pronounced. *p*-Cymene had a

234    relatively constant mixing ratio for most of the day but was elevated from mid-morning to

235    mid-afternoon. Hexanals, MBO, *p*-cymene, MT137 and estragole mixing ratios were below

236    calculated LOD, although all showed discernible daily patterns within a narrow variability

237    band, and have therefore been presented. It is possible that the reliability of removal of the

238    compounds was not consistent, resulting in high LOD. Diurnal profiles of VOC mixing ratios

239    for the second half of the campaign (Figure S8) were lower than during the first half and

240    showed similar diurnal trends. Within the limitations of the methodology described in the

241    Supplementary Information, the GC-MS measurements showed general consistency in the

242    daily pattern and magnitude of mixing ratios for the pinenes (Figure S10) with those

243    determined by PTR-MS.

244

245    **3.2.1 Wind direction/speed trends**

246    To aid identification of geographic origins of potential VOC sources, Figure S9 shows

247    bivariate polar plots of VOC mixing ratio as a function of wind speed and direction,

248    combining data from both halves of the campaign. The bivariate plots for most compounds

249    were similar, with greater mixing ratios when the wind was from S or NE, particularly for

250    high wind speeds (suggesting contributions from distant sources). Additionally, more

251    localised sources from the S, when wind speeds were lower, were particularly evident for

252    acetone, and for all other compounds. With the exception of acetaldehyde, acetone and

253    methanol, mixing ratios were also elevated for the NW wind direction, coinciding with higher

254    air temperatures. Greatest mixing ratios of *p*-cymene were observed for winds from the NW,

255    the only compound with a bivariate pattern notably different to all others.

256

257    Forest surrounds the site for several km in all directions except for a large expanse of heather

258    1.5 km to the E. The nearest sizable urban area is 6 km NW near Ermelo and Putten. On a

259    wider scale, Speuld lies within an area of land mostly covered by deciduous forest and natural

260    vegetation (Figure S1) extending 50 km N-S and covering an area of ~870 km$^2$ (Clevers et al.,

261    2007). Outside the wider forested area, a large area of agricultural land covering most of the

262    Flevopolder region (970 km$^2$) lies 15 km NW. Amsterdam is ~55 km WNW. At a horizontal

263    wind speed of 2 m s$^{-1}$ it would take less than 8 h to travel this distance, which is much shorter

264    than some of the typical atmospheric lifetimes of measured compounds, including methanol,

265    acetaldehyde, acetone, TMA and MVK (as summarised in Table S1).

266

267     It is likely that the tendency for high mixing ratios in N and S directions is due to the wider

268     forested area, as this is the most dominant land use in these directions. Of compounds also

269     showing high mixing ratios from the NW sector, TMA and hexanals have lifetimes of the

270     order of several hours, therefore the Flevopolder region may be a source of these compounds.

271     Animal husbandry is cited as the main source of atmospheric TMA (Ge et al., 2011) with

272     slurry application a minor contributor (Kuhn et al., 2011), and hexanals are known to be

273     emitted during grass cutting (Davison et al., 2008; Karl et al., 2005b).

274

275     Greater *p*-cymene mixing ratios from the NW may also be due to these sources, although *p*-

276     cymene emission is more commonly associated with deciduous broadleaf forests (Geron et

277     al., 2000). Alternatively, as *p*-cymene is detected at the same *m*/*z* as toluene (normally from

278     anthropogenic sources), it may be possible that it is the latter which was detected. Possible

279     sources could have been urban centres such as Putten/Ermelo or, further afield, Amsterdam,

280     which is feasible for this compound's relatively long lifetime (2.4 day for $1.5 \times 10^6$ cm$^{-3}$ OH).

281

282     **3.3 In-canopy mixing ratios**

283     Plots visualising the within-canopy vertical variation in the mixing ratios determined by PTR-

284     MS, as a function of time of day, are shown in Figure 3. Mixing ratios were generally higher

285     than those measured above-canopy (Figures 2 and S8). All compounds displayed similar

286     diurnal patterns to those observed for above-canopy measurements, with mixing ratios

287     increasing throughout the second half of the day. Maxima were at ~18:00, corresponding to

288     reduced vertical mixing and continued temperature-dependant emissions.

289

290     Methanol, acetaldehyde, acetone, isoprene, monoterpenes and hexanals exhibited peak mixing

291     ratios within the canopy at ~18:00, with distinct minima around 06:00 for all except

292 monoterpenes (minimum ~13:00). Isoprene mixing ratios decreased more rapidly than for

293 other compounds, reaching the minimum by midnight. Acetaldehyde, acetone and

294 monoterpenes had particularly elevated mixing ratios toward the bottom of the canopy (5-10

295 m), as had been observed for monoterpenes during previous work (Dorsey et al., 2004). This

296 may be due to large quantities of leaf litter on the forest floor acting as a source.

297

298 MVK + MACR, MBO and estragole had peak mixing ratios at the top of the canopy. For

299 MVK + MACR this can be explained by formation in-canopy from oxidation of isoprene,

300 rather than primary emission, therefore peak mixing ratio coincides with highest PAR at the

301 top of the canopy. Pine species are reported a source of MBO (Harley et al., 1998) with

302 emission dependant on both light and temperature (Holzinger et al., 2005). Estragole emission

303 occurs via both storage pools (similar to monoterpenes) and directly after synthesis in a light

304 and temperature driven mechanism (similar to MBO) (Bouvier-Brown et al., 2009). Increased

305 PAR higher in the canopy may therefore explain mixing ratio profiles of these compounds,

306 while storage pool emissions of estragole result in a slower decline in mixing ratios overnight.

307

308 TMA and *p*-cymene profiles differed from all others and were less structured. TMA mixing

309 ratios were, in general, greater towards the top of the canopy, except for ~18:00 when mixing

310 ratios were elevated at all heights. Mixing ratios also remained high overnight. Peak *p*-

311 cymene mixing ratios were between 22:00 and 06:00 low in the canopy (5-10 m).

312

313 The GC-MS data presented in the Supplementary Information support the observations from

314 the in-canopy PTR-MS measurements that total measured monoterpene mixing ratios

315 (comprising α- and β-pinene, 3-carene and limonene) were generally larger at lower heights

316 (Figure S11), similar to a previous study at the Speuld site (Peters et al., 1994). In-canopy (4

13

317   and 18 m) mixing ratios were highest in the morning and evening and lowest in the afternoon,

318   with largest afternoon mixing ratios at the top of the canopy (32 m) and above (40 m). The

319   four measured monoterpenes are consistent with Lerdau et al. (1995) who reported that α-

320   pinene, β-pinene and 3-carene account for 95 % monoterpene emissions from Douglas fir. α-

321   Pinene is the dominant monoterpene at all heights within and above the canopy (Figure S12).

322

323   **4 Discussion**

324

325   **4.1 Terpenoids**

326   Monoterpene mixing ratios observed in this work are in agreement with previous observations

327   at the site (Dorsey et al., 2004; Peters et al., 1994). They were generally larger at night,

328   peaking at 23:30 (1.76 ppbv) and 16:00 (0.95 ppbv) during the first and second halves of the

329   campaign, respectively, and larger closer to the forest floor, suggesting a source contribution

330   low in the canopy such as the large quantities of leaf litter.

331

332   Monoterpene fluxes from vegetation have been shown to increase exponentially with

333   temperature (Guenther et al., 1993; Pressley et al., 2004), according to the G93 algorithm,

334   $$E_{meas} = E_s e^{[\beta(T-T_s)]} \tag{1}$$

335   where $E_{meas}$ is measured emission rate at leaf temperature $T$ (°C), $E_s$ is the standard emission

336   rate at 30 °C ($T_s$) and $\beta$ is an empirical temperature coefficient. To convert from an area flux

337   to a foliar mass flux a foliar density $D$ of 600 $g_{dw}$ m$^{-2}$ was assumed for *Pseudotsuga spp.*

338   (Guenther et al., 1994). See below for comment on uncertainty in this value. The canopy

339   temperature was not directly measured so a sensitivity of the derived standardised

340   monoterpene flux to this temperature parameter was undertaken. Using Equation (1) and

341   above-canopy temperature the standard monoterpene emission rates for the two halves of the

342    campaign were calculated to be $1.0 \pm 0.5$ and $0.9 \pm 0.2$ µg $g_{dw}^{-1}$ $h^{-1}$, with temperature

343    coefficients of $0.19 \pm 0.06$ and $0.08 \pm 0.05$ $°C^{-1}$, respectively. For these measurements in

344    temperate latitudes it is anticipated that the canopy temperature is in the range around 2 K

345    higher than the above-canopy temperature, which decreases the derived standardised emission

346    rates to $0.8 \pm 0.3$ and $0.8 \pm 0.2$ µg $g_{dw}^{-1}$ $h^{-1}$ for the two halves of the campaign, respectively.

347    (Same temperature coefficients.) These latter standardised monoterpene fluxes are well within

348    the uncertainties of the previously-calculated standardised fluxes but because of the

349    systematic nature of the effect of temperature these latter fluxes are taken as the better

350    estimates. Realistic levels of uncertainty in the temperature parameter will not alter the

351    calculated emission rates outside of the large uncertainty ranges that are already associated

352    with deriving these values from the measurement data.

353

354    Uncertainty in the value of $D$ contributes further uncertainty to the derived emission rates.

355    Anticipating that relative uncertainty in $D$ is within 20% modifies the statistical uncertainty

356    ranges for the standard MT emission rates in the two halves of the campaign to $0.8 \pm 0.4$ and

357    $0.8 \pm 0.3$ µg $g_{dw}^{-1}$ $h^{-1}$. The standardised values are compared with other Douglas fir studies in

358    Table 2. The large statistical standard deviations in the derived parameters reflect the scatter

359    in the relationships between $E_{meas}$ and $T$ observed in this work ($R^2 = 0.29$ and $0.17$ for the first

360    and second halves of the campaign, respectively), which is likely due to noisy flux data and

361    being close to instrument LOD. The second half of the campaign also has only half the

362    number of above-canopy flux data because of the interspersed in-canopy measurements. The

363    standard monoterpene emission factors from this study are within the range of previously

364    derived values for *P. menziesii*. All other studies used branch enclosure methods. Short-

365    duration temperature and light differences within the canopy would lead to deviations of

366    canopy-scale averages from enclosure studies. The temperature coefficients derived from the

367  two halves of the study although differing by more than a factor of two are not statistically

368  significant different because of the large uncertainties, and are in line with the generally

369  accepted value for most plants (Guenther et al., 1993).

370

371  Although Douglas fir trees – and coniferous species in general – are thought to be non-

372  emitters of isoprene, fluxes were discernible, as they were for isoprene oxidation products

373  MVK + MACR. The above-canopy mixing ratios of these species exhibited a diurnal pattern

374  throughout the campaign. Figure 3 shows that elevated isoprene mixing ratios occurred

375  throughout the canopy, whilst maximum MVK + MACR mixing ratios were at the top of the

376  canopy, ~32 m. This supports the forest canopy as a source of isoprene, which is oxidised to

377  form MVK and MACR, peaking at the canopy top where PAR is greatest. As isoprene

378  emission from plants is strongly influenced by light and temperature, the canopy-level

379  emission, $F$, was recalculated as a standard emission factor ($\varepsilon$) for a leaf temperature of 303 K

380  and PAR flux of 1000 μmol m$^{-2}$ s$^{-1}$, as described by the G95 algorithm (Guenther et al.,

381  1995),

382  $$\varepsilon = \frac{F}{D\,\gamma} \qquad (2)$$

383  where $D$ is foliar density (g$_{dw}$ m$^{-2}$) and $\gamma$ is a non-dimensional activity adjustment factor to

384  account for effects of light and temperature:

385  $$\gamma = C_L C_T \qquad (3)$$

386  The light dependence, $C_L$, is defined by

387  $$C_L = \frac{\alpha C_L Q}{\sqrt{1+\alpha^2 Q^2}} \qquad (4)$$

388  where $\alpha$ (0.0027) and $c_{L1}$ (1.066) are empirical coefficients and $Q$ is PAR flux (μmol m$^{-2}$ s$^{-1}$).

389  The temperature dependence $C_T$, is defined by

16

$$390 \qquad C_T = \frac{exp\frac{c_{T1}(T-T_S)}{RT_ST}}{1+exp\frac{(c_{T2}(T-T_M))}{RT_ST}} \qquad (5)$$

391    where $T$ is leaf temperature (K), $T_s$ is leaf temperature at standard conditions (303 K), $R$ is the

392    universal gas constant (8.314 J K$^{-1}$ mol$^{-1}$), and $c_{T1}$ (95 kJ mol$^{-1}$), $c_{T2}$ (230 kJ mol$^{-1}$) and $T_M$

393    (314 K) are empirical coefficients.

394

395    Hourly values of above-canopy PAR and temperature, and of isoprene flux (from Figures 1

396    and S6), were used to calculate $\gamma$ and $F$ respectively. As above, a 2 K enhancement of ambient

397    temperature was assumed as a better proxy of canopy temperature, and also as above a foliar

398    density of 600 g$_{dw}$ m$^{-2}$ was used. Hourly emission factors $\varepsilon$ were then determined for isoprene

399    for the first and second halves of the campaign, and these had peak values of 0.64 and 0.62 µg

400    g$_{dw}$$^{-1}$ h$^{-1}$, respectively. Mean daytime standard values of 0.09 ± 0.12 and 0.16 ± 0.18 µg g$_{dw}$$^{-1}$

401    h$^{-1}$ were calculated to allow comparison in Table 2 with mean values from other studies.

402    These flux values are also subject to uncertainty from the assumed foliar density which we

403    anticipate should be within 20%. Standard isoprene emission factors from this study were at

404    the low end previously derived values for *Pseudotsuga spp.*, but the values here are canopy

405    scale rather than branch scale and variability quoted in all measurements is large.

406

407    **4.2 Non-terpenoids**

408    Non-terpenoids were investigated for the first time at the Speuld site. Only one previous study

409    could be found which qualitatively measured other VOCs from Douglas fir saplings (Joó et

410    al., 2011). Positive fluxes were observed for all compounds determined except TMA and *p*-

411    cymene (and/or toluene) which exhibited net deposition. Maximum daily median fluxes of

412    some oxygenated compounds were larger than from other coniferous studies. Methanol and

413    acetaldehyde fluxes (2.6 and 0.7 mg m$^{-2}$ h$^{-1}$, respectively (Figure S6) were larger than those

414 measured in a subalpine, coniferous forest in USA where fluxes peaked at 1 and 0.4 mg m$^{-2}$ h$^{-1}$

415 , respectively (Karl et al., 2002). Acetone fluxes were identical at both sites (0.8 mg m$^{-2}$ h$^{-1}$).

416 Methanol, acetaldehyde and acetone fluxes at Speuld were also higher than those above a

417 Scots pine canopy in Finland (0.4, 0.15 and 0.3 mg m$^{-2}$ h$^{-1}$, respectively (Rinne et al., 2007)).

418 In both studies, measurements were carried out during summer (June and July, respectively).

419 Daily temperatures at the subalpine site in USA peaked at ~17 °C. In contrast, peak

420 temperatures at the Finnish site were only slightly cooler (~25 °C) than at Speuld but night-

421 time minimum temperatures were much cooler (~14 °C). Higher temperatures at Speuld may

422 therefore account for the larger measured fluxes here than at these other locations.

423

424 In-canopy mixing ratios further support Douglas fir as a source of methanol, acetaldehyde,

425 acetone, hexanals, MBO and estragole. It has been shown in several studies that decaying

426 plant material is a source of oxygenated VOCs, such as ponderosa pine (Schade and

427 Goldstein, 2001), loblolly pine (Karl et al., 2005a) and decaying spruce needles (Warneke et

428 al., 1999). As there was a thick layer of leaf litter on the forest floor, it is feasible that this was

429 a source of oxygenated VOCs, particularly acetaldehyde and acetone which had highest

430 mixing ratios near the forest floor.

431

432 Above-canopy mixing ratios of all VOCs followed a similar diurnal trend of maxima in the

433 evening or at night, with methanol, acetaldehyde, acetone, TMA, isoprene and MVK +

434 MACR all above LOD. This can be explained by reduced radical sink chemistry at night,

435 coupled with reduced vertical mixing, resulting in accumulation within a shallower boundary

436 layer.

437

18

438     Mixing ratios of all compounds appeared to be predominantly influenced by the wider

439     forested area, with more distant sources also identified, particularly for TMA and *p*-cymene.

440     Arable and grass land NW of the site was thought to be a source of elevated TMA mixing

441     ratios. Elevated mixing ratios at *m*/*z* 93 were potentially attributable to anthropogenic toluene,

442     as evidenced from Figure S9 which shows elevated mixing ratios associated with urban areas

443     in the WNW direction. These PTR-MS measurements were unable to discriminate different

444     compounds with identical *m*/*z*.

445

446     **5 Conclusions**

447     Fluxes and mixing ratios of VOC were measured by PTR-MS and vDEC at a Douglas fir

448     forest in Speuld, The Netherlands. Monoterpene fluxes were comparable with other studies of

449     Douglas fir, with calculated standard emission factor of $0.8 \pm 0.4$ and $0.8 \pm 0.3$ $\mu$g $g_{dw}^{-1}$ $h^{-1}$,

450     and temperature coefficients of $0.19 \pm 0.06$ and $0.08 \pm 0.05$ $°C^{-1}$ for the first and second

451     halves of the campaign, respectively. Mean standard emission factors for isoprene were 0.09

452     $\pm 0.12$ and $0.16 \pm 0.18$ $\mu$g $g_{dw}^{-1}$ $h^{-1}$ for the two halves respectively.

453

454     Fluxes of several non-terpenoid VOCs were significant, with maximum fluxes greater than

455     has been measured for other coniferous species. α-Pinene was the dominant monoterpene

456     within and above the canopy. Within canopy mixing ratios of individual species were

457     generally greatest in early evening consistent with reduced vertical mixing and continued

458     temperature-dependent emissions. Acetaldehyde, acetone and monoterpenes had elevated

459     mixing ratios toward the bottom of the canopy (5-10 m) with likely contribution from the

460     large quantities of forest-floor leaf litter. MBO and estragole had peak mixing ratios at the top

461     of the canopy and are known to have coniferous sources. MVK + MACR also had highest

462     mixing ratios at the top of the canopy consistent with formation from in-canopy oxidation of

19

463    isoprene. The work highlights the importance of quantifying a wider variety of VOCs from

464    biogenic sources than isoprene and monoterpenes.

465

474

475 **References**

476

477 Ammann, C., Brunner, A., Spirig, C., Neftel, A., 2006. Technical note: Water vapour

478 concentration and flux measurements with PTR-MS. Atmospheric Chemistry and Physics 6,

479 4643-4651.

480 Arey, J., Crowley, D. E., Crowley, M., Resketo, M., Lester, J., 1995. Hydrocarbon Emissions

481 from Natural Vegetation in California South-Coast-Air-Basin. Atmospheric Environment 29,

482 2977-2988.

483 Blake, R. S., Monks, P. S., Ellis, A. M., 2009. Proton-Transfer Reaction Mass Spectrometry.

484 Chemical Reviews 109, 861-896.

485 Bouvier-Brown, N. C., Goldstein, A. H., Worton, D. R., Matross, D. M., Gilman, J. B.,

486 Kuster, W. C., Welsh-Bon, D., Warneke, C., de Gouw, J. A., Cahill, T. M., Holzinger, R.,

487 2009. Methyl chavicol: characterization of its biogenic emission rate, abundance, and

488 oxidation products in the atmosphere. Atmospheric Chemistry and Physics 9, 2061-2074.

489 Clevers, J., Schaepman, M., Mucher, C., De Wit, A., Zurita-Milla, R., Bartholomeus, H.,

490 2007. Using MERIS on Envisat for land cover mapping in the Netherlands. International

491 Journal of Remote Sensing 28, 637-652.

492 Copeland, N., Cape, J. N., Heal, M. R., 2012. Volatile organic compound emissions from

493 *Miscanthus* and short rotation coppice willow bioenergy crops. Atmospheric Environment 60,

494 327-335.

495 Davison, B., Brunner, A., Ammann, C., Spirig, C., Jocher, M., Neftel, A., 2008. Cut-induced

496 VOC emissions from agricultural grasslands. Plant Biology 10, 76-85.

497 Dorsey, J. R., Duyzer, J. H., Gallagher, M. W., Coe, H., Pilegaard, K., Weststrate, J. H.,

498 Jensen, N. O., Walton, S., 2004. Oxidized nitrogen and ozone interaction with forests. I:

499 Experimental observations and analysis of exchange with Douglas fir. Quarterly Journal of

500 the Royal Meteorological Society 130, 1941-1955.

501  Drewitt, G. B., Curren, K., Steyn, D. G., Gillespie, T. J., Niki, H., 1998. Measurement of
502  biogenic hydrocarbon emissions from vegetation in the lower Fraser valley, British Columbia.
503  Atmospheric Environment 32, 3457-3466.

504  Ge, X., Wexler, A. S., Clegg, S. L., 2011. Atmospheric amines - Part I. A review.
505  Atmospheric Environment 45, 524-546.

506  Geron, C., Rasmussen, R., Arnts, R. R., Guenther, A., 2000. A review and synthesis of
507  monoterpene speciation from forests in the United States. Atmospheric Environment 34,
508  1761-1781.

509  Guenther, A., Hewitt, C. N., Erickson, D., et al , 1995. A global model of natural volatile
510  organic compound emissions. Journal of Geophysical Research 100, 8873-8892.

511  Guenther, A., Karl, T., Harley, P., Wiedinmyer, C., Palmer, P. I., Geron, C., 2006. Estimates
512  of global terrestrial isoprene emissions using MEGAN (Model of Emissions of Gases and
513  Aerosols from Nature). Atmospheric Chemistry and Physics 6, 3181-3210.

514  Guenther, A., Zimmerman, P., Wildermuth, M., 1994. Natural Volatile Organic-Compound
515  Emission Rate Estimates for United-States Woodland Landscapes. Atmospheric Environment
516  28, 1197-1210.

517  Guenther, A. B., Zimmerman, P. R., Harley, P. C., Monson, R. K., Fall, R., 1993. Isoprene
518  and Monoterpene Emission Rate Variability - Model Evaluations and Sensitivity Analyses.
519  Journal of Geophysical Research 98, 12609-12617.

520  Harley, P., Fridd-Stroud, V., Greenberg, J., Guenther, A., Vasconcellos, P., 1998. Emission of
521  2-methyl-3-buten-2-ol by pines: A potentially large natural source of reactive carbon to the
522  atmosphere. Journal of Geophysical Research-Atmospheres 103, 25479-25486.

523  Holzinger, R., Lee, A., Paw, K. T., Goldstein, A. H., 2005. Observations of oxidation
524  products above a forest imply biogenic emissions of very reactive compounds. Atmospheric
525  Chemistry and Physics 5, 67-75.

526    Joó, E., Dewulf, J., Amelynck, C., Schoon, N., Pokorska, O., Simpraga, M., Steppe, K.,

527    Aubinet, M., Van Langenhove, H., 2011. Constitutive versus heat and biotic stress induced

528    BVOC emissions in *Pseudotsuga menziesii*. Atmospheric Environment 45, 3655-3662.

529    Karl, M., Guenther, A., Koble, R., Leip, A., Seufert, G., 2009. A new European plant-specific

530    emission inventory of biogenic volatile organic compounds for use in atmospheric transport

531    models. Biogeosciences 6, 1059-1087.

532    Karl, T., Hansel, A., Mark, T., Lindinger, W., Hoffmann, D., 2003. Trace gas monitoring at

533    the Mauna Loa Baseline observatory using proton-transfer reaction mass spectrometry.

534    International Journal of Mass Spectrometry 223, 527-538.

535    Karl, T., Harley, P., Guenther, A., Rasmussen, R., Baker, B., Jardine, K., Nemitz, E., 2005a.

536    The bi-directional exchange of oxygenated VOCs between a loblolly pine (*Pinus taeda*)

537    plantation and the atmosphere. Atmospheric Chemistry and Physics 5, 3015-3031.

538    Karl, T., Harren, F., Warneke, C., de Gouw, J., Grayless, C., Fall, R., 2005b. Senescing grass

539    crops as regional sources of reactive volatile organic compounds. Journal of Geophysical

540    Research-Atmospheres 110, D15302, doi:10.1029/2005JD005777 .

541    Karl, T. G., Spirig, C., Rinne, J., Stroud, C., Prevost, P., Greenberg, J., Fall, R., Guenther, A.,

542    2002. Virtual disjunct eddy covariance measurements of organic compound fluxes from a

543    subalpine forest using proton transfer reaction mass spectrometry. Atmospheric Chemistry

544    and Physics 2, 279-291.

545    Kesselmeier, J., Staudt, M., 1999. Biogenic volatile organic compounds (VOC): An overview

546    on emission, physiology and ecology. Journal of Atmospheric Chemistry 33, 23-88.

547    Kljun, N., Calanca, P., Rotachhi, M. W., Schmid, H. P., 2004. A simple parameterisation for

548    flux footprint predictions. Boundary-Layer Meteorology 112, 503-523.

549    Kuhn, U., Sintermann, J., Spirig, C., Jocher, M., Ammann, C., Neftel, A., 2011. Basic

550    biogenic aerosol precursors: Agricultural source attribution of volatile amines revised.

551    Geophysical Research Letters 38, L16811, doi:10.1029/2011GL047958.

552    Lerdau, M., Matson, P., Fall, R., Monson, R., 1995. Ecological Controls Over Monoterpene

553    Emissions from Douglas-Fir (*Pseudotsuga-Menziesii*). Ecology 76, 2640-2647.

554    Misztal, P. K., Nemitz, E., Langford, B., Di Marco, C. F., Phillips, G. J., Hewitt, C. N.,

555    MacKenzie, A. R., Owen, S. M., Fowler, D., Heal, M. R., Cape, J. N., 2011. Direct ecosystem

556    fluxes of volatile organic compounds from oil palms in South-East Asia. Atmospheric

557    Chemistry and Physics 11, 8995-9017.

558    Misztal, P. K., Owen, S. M., Guenther, A. B., Rasmussen, R., Geron, C., Harley, P., Phillips,

559    G. J., Ryan, A., Edwards, D. P., Hewitt, C. N., Nemitz, E., Siong, J., Heal, M. R., Cape, J. N.,

560    2010. Large estragole fluxes from oil palms in Borneo. Atmospheric Chemistry and Physics

561    10, 4343-4358, doi:10.5194/acp-10-4343-2010.

562    Peters, R. J. B., Duivenbode, J. A. D. V., Duyzer, J. H., Verhagen, H. L. M., 1994. The

563    determination of terpenes in foreset air. Atmospheric Environment 28, 2413-2419.

564    Pressley, S., Lamb, B., Westberg, H., Guenther, A., Chen, J., Allwine, E., 2004. Monoterpene

565    emissions from a Pacific Northwest Old-Growth Forest and impact on regional biogenic VOC

566    emission estimates. Atmospheric Environment 38, 3089-3098.

567    Rinne, H. J. I., Guenther, A. B., Warneke, C., de Gouw, J. A., Luxembourg, S. L., 2001.

568    Disjunct eddy covariance technique for trace gas flux measurements. Geophysical Research

569    Letters 28, 3139-3142.

570    Rinne, J., Taipale, R., Markkanen, T., Ruuskanen, T., Hellen, H., Kajos, M., Vesala, T.,

571    Kulmala, M., 2007. Hydrocarbon fluxes above a Scots pine forest canopy: measurements and

572    modeling. Atmospheric Chemistry and Physics 7, 3361-3372.

573    Schade, G. W., Goldstein, A. H., 2001. Fluxes of oxygenated volatile organic compounds

574    from a ponderosa pine plantation. Journal of Geophysical Research-Atmospheres 106, 3111-

575    3123.

576    Steiner, A. H., Goldstein, A. L., 2007. Biogenic VOCs, in *Volatile organic compounds in the*

577    *atmosphere*, (ed. Koppmann, R.), Wiley-Blackwell.

578 Taipale, R., Ruuskanen, T., Rinne, J., Kajos, M., Hakola, H., Pohja, T., Kulmala, M., 2008.

579 Technical Note: Quantitative long-term measurements of VOC concentrations by PTR-MS -

580 measurement, calibration, and volume mixing ratio calculation methods. Atmospheric

581 Chemistry and Physics 8, 6681-6698.

582 Warneke, C., Karl, T., Judmaier, H., Hansel, A., Jordan, A., Lindinger, W., Crutzen, P. J.,

583 1999. Acetone, methanol, and other partially oxidized volatile organic emissions from dead

584 plant matter by abiological processes: Significance for atmospheric HOx chemistry. Global

585 Biogeochemical Cycles 13, 9-17.

586

587

**Tables**

Table 1: Compounds measured during this study, with dwell times, sensitivities and limits of detection during the two halves of the measurement period.

| $m/z$ [amu] | Contributing compound(s) | Formula | Dwell time [s] | Sensitivity [ncps ppbv$^{-1}$] | Limit of detection [ppbv] | |
|---|---|---|---|---|---|---|
| | | | | | First half | Second half |
| 21 | water isotope | $H_2^{18}O$ | 0.2 | - | - | - |
| 33 | methanol | $CH_4O$ | 0.5 | 9.53 | 0.58 | 0.95 |
| 37 | water cluster | $(H_2O)_2$ | 0.2 | - | - | - |
| 45 | acetaldehyde | $C_2H_4O$ | 0.5 | 11.1 | 0.21 | 0.27 |
| 59 | acetone | $C_3H_6O$ | 0.5 | 10.1 | 0.10 | 0.11 |
| | propanal | | | | | |
| 60 | trimethylamine (TMA) | $N(CH_3)_3$ | 0.5 | 8.25 | 0.09 | 0.13 |
| 69 | isoprene | $C_5H_8$ | 0.5 | 2.42 | 0.24 | 0.26 |
| | furan | | | | | |
| | methyl butenol fragment | | | | | |
| 71 | methyl vinyl ketone (MVK) | $C_4H_6O$ | 0.5 | 4.84 | 0.13 | 0.14 |
| | methacrolein (MACR) | | | | | |
| 81 | monoterpene fragment (MT81) | | 0.5 | 1.9 | 0.36 | 0.28 |
| 83 | (Z)-3-hexenol fragment | | 0.5 | 1.1 | 0.69 | 0.60 |
| | (E)-3-hexenol fragment | | | | | |
| | (E)-2-hexenol fragment | | | | | |
| | hexanal fragment | | | | | |
| | (E,Z)-2-hexenyl acetate fragment | | | | | |
| 87 | 2-methyl-3-buten-2-ol (MBO) | $C_5H_{10}O$ | 0.5 | 1 | 0.65 | 0.71 |
| 93 | *p*-cymene fragment | $C_7H_8$ | 0.5 | 0.9 | 1.08 | 0.69 |
| | toluene | | | | | |
| 137 | monoterpene (MT137) | $C_{10}H_{16}$ | 0.5 | 0.235 | 3.03 | 2.44 |
| 149 | estragole | $C_{10}H_{12}O$ | 0.5 | 0.2 | 3.77 | 5.55 |

Table 2: Comparison of standardised emission rates of monoterpenes and isoprene from Douglas fir.

| Species | Monoterpenes / $\mu g\ g_{dw}^{-1}\ h^{-1}$ | Temperature coefficient / $°C^{-1}$ | Isoprene / $\mu g\ g_{dw}^{-1}\ h^{-1}$ | Measurement type | Reference |
|---|---|---|---|---|---|
| *Pseudotsuga menziesii* | 0.8 ± 0.4<br>0.8 ± 0.3 | 0.19 ± 0.06<br>0.08 ± 0.05 | 0.09 ± 0.12<br>0.16 ± 0.18 | Canopy-scale, PTR-MS | This study, first half<br>This study, second half |
| " | 0.44 ± 0.16 | 0.14 ± 0.05 | | Dynamic branch enclosure, mature forest | Pressley et al. (2004) |
| " | 0.8 ± 0.2 (healthy)<br>6.8 (stressed) | 0.133 ± 0.013 (healthy)<br>0.316 (stressed) | | Dynamic branch enclosure, saplings | Joó et al. (2011) |
| " | 1.81 | | <0.11 | - | Guenther et al. (1994) |
| " | 2.0 | | 1.0 | - | Karl et al. (2009) |
| " | 2.3 ± 1.4 | | 1.5 ± 1.6 | - | Kesselmeir and Staudt (1999) |
| " | 2.60 ± 1.63 | assumed to be 0.09 ± 0.025 | 1.72 ± 1.85 | Dynamic branch enclosure, mature trees | Drewitt et al. (1998) |
| *Pseudotsuga macrocarpa* | 1.1 ± 0.3 | | 0.0 | Dynamic branch enclosure, immature tree (greenhouse) | Arey et al. (1995) |

588

# Figures

Figure 1: Average diurnal profiles of VOC fluxes above Douglas fir and of sensible heat flux, prior to 20:00 on 29th June 2009. Data points are the mean of median values for a ±1.5 hour time window. Note the variable scales. Grey areas show variability calculated as ±1 sd.



28
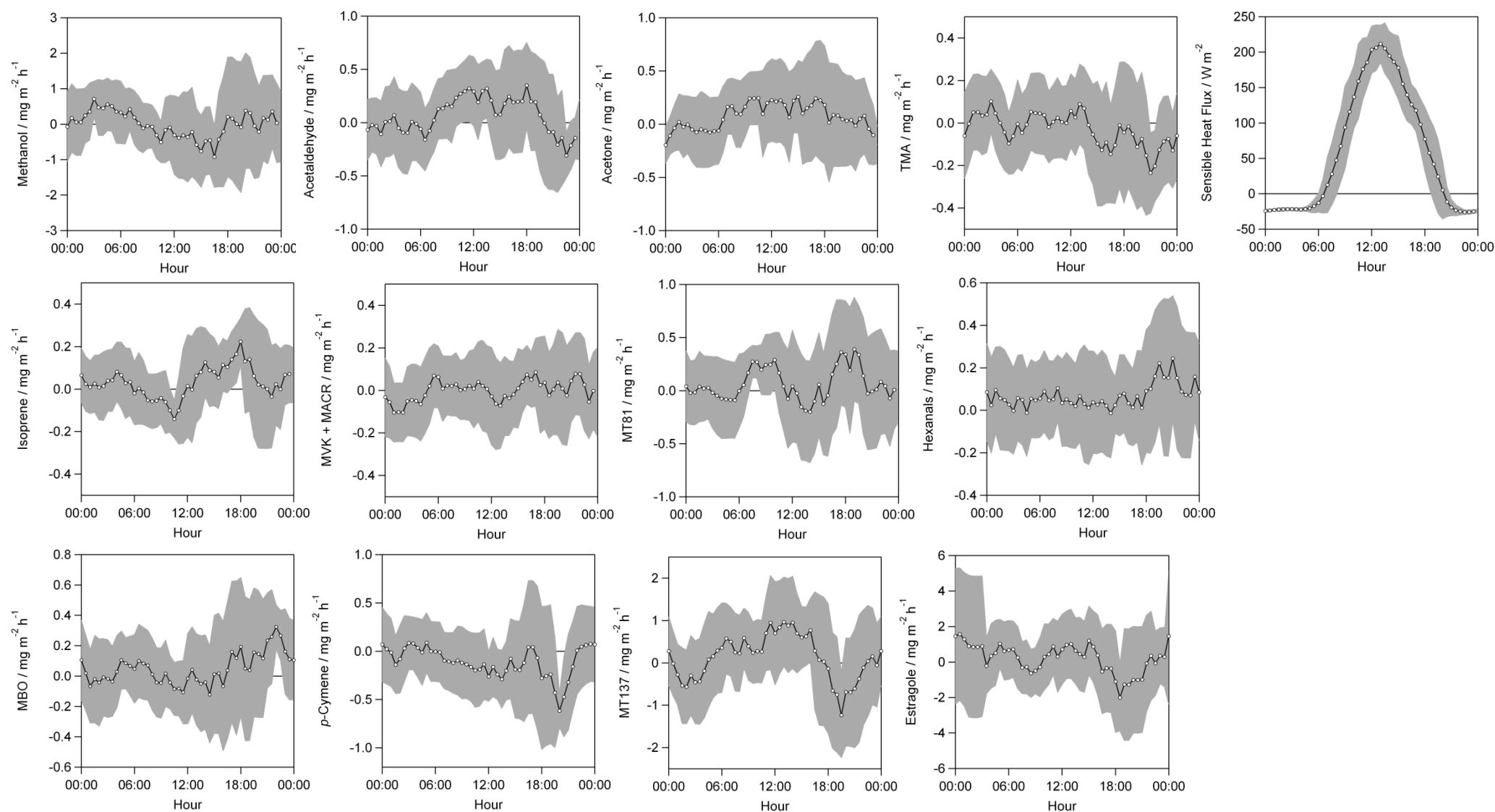
Figure 2: Average diurnal profiles of VOC mixing ratios above Douglas fir, and of temperature, before 20:00 on 29 June 2009. Note the variable scales. Dashed lines denote LOD. Grey areas show variability calculated as ±1 sd of the averaged half-hourly values of all measurements.
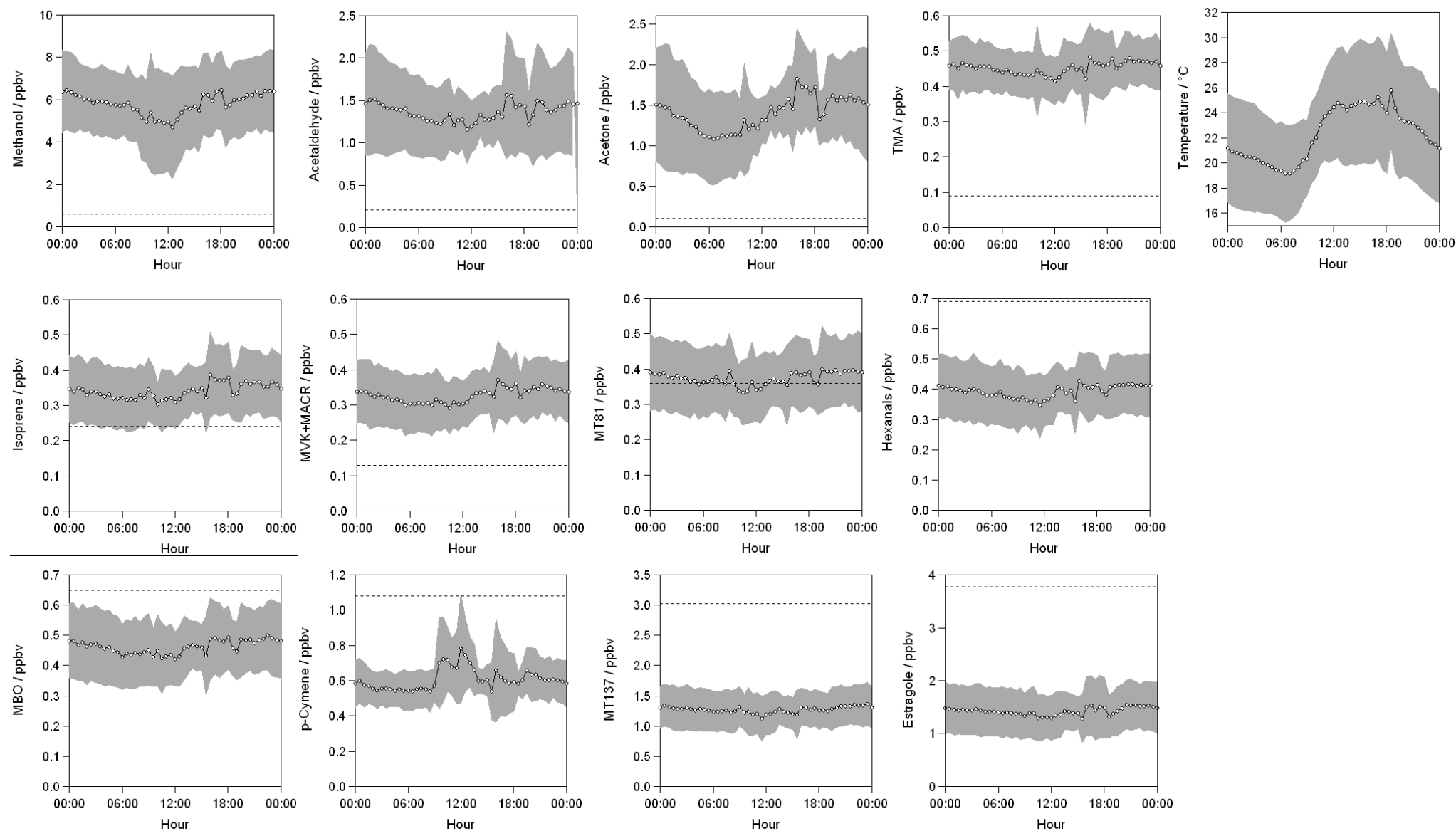
Figure 3: Within-canopy mixing ratios (ppbv, denoted by colour) as a function of time of day (hour, x-axis) and canopy height above ground (m, y-axis). Note the variable scales.
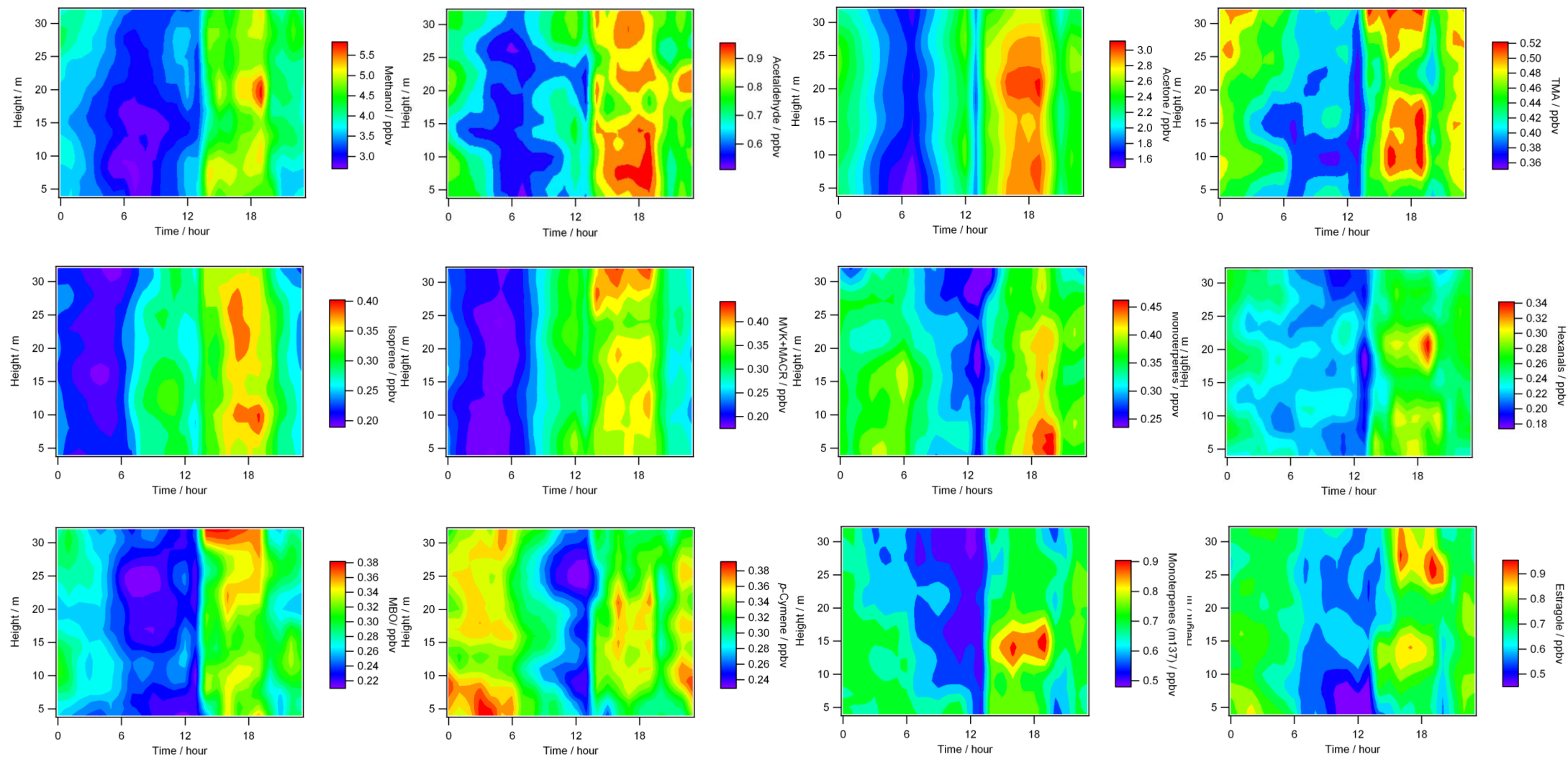
**Volatile organic compound speciation above and within a Douglas Fir forest**


Nichola Copeland[1,2], J. Neil Cape[1], Eiko Nemitz, Mathew R. Heal[2]


[1] Centre for Ecology & Hydrology, Bush Estate, Penicuik, EH26 0QB, UK

[2] EaStChem School of Chemistry, University of Edinburgh, West Mains Road, Edinburgh, EH9 3JJ, UK


**Contents**

Table S1: Atmospheric lifetimes of all compounds measured in this work.

| Compound(s) | | Atmospheric lifetimes | | |
|---|---|---|---|---|
| | | OH | $O_3$ | $NO_3$ |
| Methanol [a] | | 15 d | | >220 d |
| Acetaldehyde [a] | | 11 h | >4.5 y | 17 d |
| Acetone [a] | | 61 d | >4.5 y | >8 y |
| Trimethylamine (TMA) [b] | | 4.6 - 7 h | 5.9 d | <53 d |
| Isoprene [a] | | 2 h | 1.3 d | 50 min |
| Methyl vinyl ketone (MVK) [a] | | 9 h | 3.6 d | |
| Methacrolein (MACR) [a] | | 5 h | 15 d | 10 d |
| Monoterpenes | α-pinene [c] | 2.6 h | 4.6 h | 11 min |
| | β-pinene [c] | 1.8 h | 1.1 d | 27 min |
| | 3-carene [c] | 1.6 h | 11 h | 7 min |
| | limonene [c] | 49 min | 2 h | 5 min |
| Hexanals [d] | | 7 h | | |
| 2-methyl-3-buten-2-ol (MBO) [e] | | 2.1 h | | |
| p-Cymene [f] | | 1 d | >330 d | 1.3 y |
| Estragole [g] | | 55 min | 18 h | |

[a] (Harrison and Hester, 1995), [OH] $1.6 \times 10^6$ cm$^{-1}$, [$O_3$] $7 \times 10^{11}$ cm$^{-1}$, [$NO_3$] $5 \times 10^8$ cm$^{-1}$

[b] (Lee and Wexler, 2013), [OH] $1 \times 10^6$ cm$^{-1}$, [$O_3$] $2.5 \times 10^{11}$ cm$^{-1}$, [$NO_3$] $5 \times 10^8$ cm$^{-1}$

[c] (Atkinson and Arey, 2003), [OH] $2 \times 10^6$ cm$^{-1}$, [$O_3$] $7 \times 10^{11}$ cm$^{-1}$, [$NO_3$] $2.5 \times 10^8$ cm$^{-1}$

[d] (Jiménez et al., 2007), [OH] $1 \times 10^6$ cm$^{-1}$

[e] (Schade and Goldstein, 2001), [OH] $2 \times 10^6$ cm$^{-1}$

[f] (Corchnoy and Atkinson, 1990), [OH] $1.5 \times 10^6$ cm$^{-1}$, [$O_3$] $7 \times 10^{11}$ cm$^{-1}$, [$NO_3$] $2.4 \times 10^8$ cm$^{-1}$

[g] (Bouvier-Brown et al., 2009), [OH] $5.4 \times 10^6$ cm$^{-1}$, [$O_3$] $1.18 \times 10^{12}$ cm$^{-1}$

Figure S1: Location of the Speulderbos measurement site in The Netherlands superimposed on a land cover map. Adapted from Figure 7 in Clevers et al. (2007).
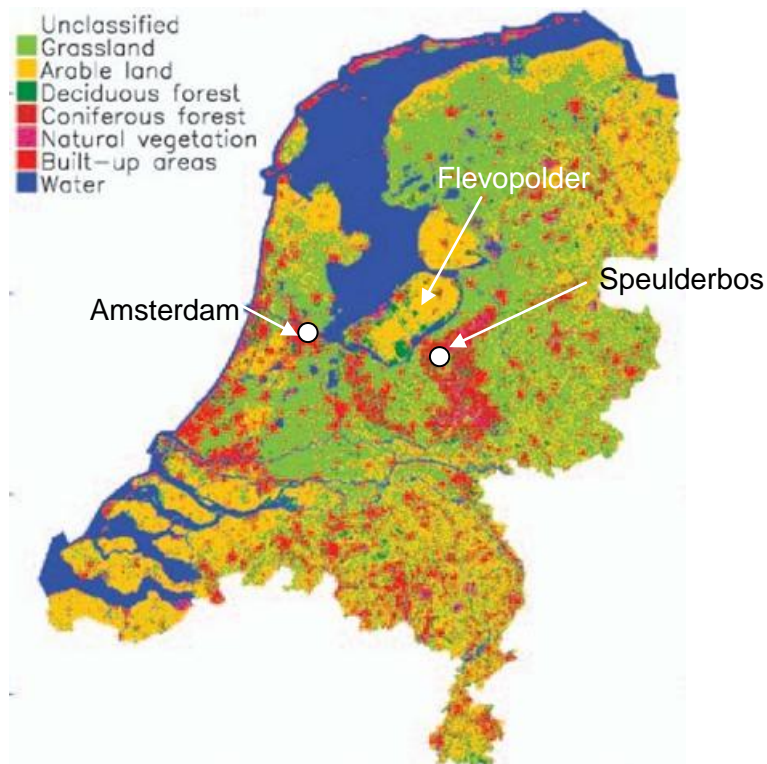


Figure S2: Aerial view of the Speuld measurement site. Grey lines show footpaths through the forest. The location of the sampling tower is indicated by the white marker. (Map attributable to ©2012 Aerodata International Surveys, Geoeye (Imagery) and ©2012 Google (map data)).

Figure S3: Modelled flux footprints for this study. The following parameters were used: measurement height $z_m$ 45 m; roughness length $z_0$ 3.2 m (estimated as 1/10th of the canopy height, 32 m); boundary layer height $h$ 1000 m. Footprints were calculated for minimum, median and maximum values of $u*$ (1 sd of the vertical wind speed, $\sigma_w$, shown in brackets) as indicated on the graph. The distance at which maximum contribution can be expected, and at which 80% of the flux is contained, are given as $X_{max}$ and $X_r$, respectively.



Legend:
- $u*$ max = 1.687 (1.421) m/s (Xmax 301.8 m, Xr 660.2 m)
- $u*$ median = 0.286 (0.538) m/s (Xmax 158.7 m, Xr 347.3 m)
- $u*$ min = 0.200 (0.408) m/s (Xmax 148.7 m, Xr 325.3 m)

y-axis: fy / m$^{-1}$ (crosswind-integrated f)

x-axis: X / m
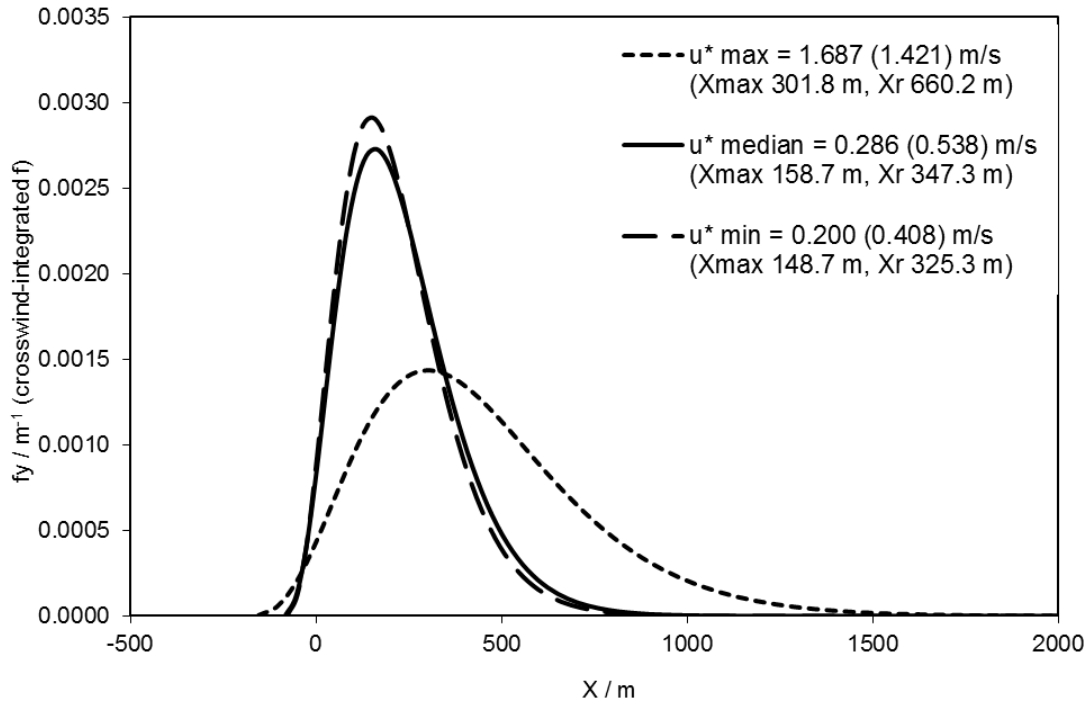
Figure S4: Map showing the predicted radius of the maximum 80% flux footprint using a simple parameterisation model (Kljun et al., 2004). The blue marker indicates the location of the sampling tower within Speuld forest. (Map data ©2012 Google Imagery ©2012 TerraMetrics. Radius plotted using www.freemaptools.com).

Figure S5: Time series of VOC fluxes measured above Douglas fir. Dashed gridlines denote midnight. Note the variable flux scales.
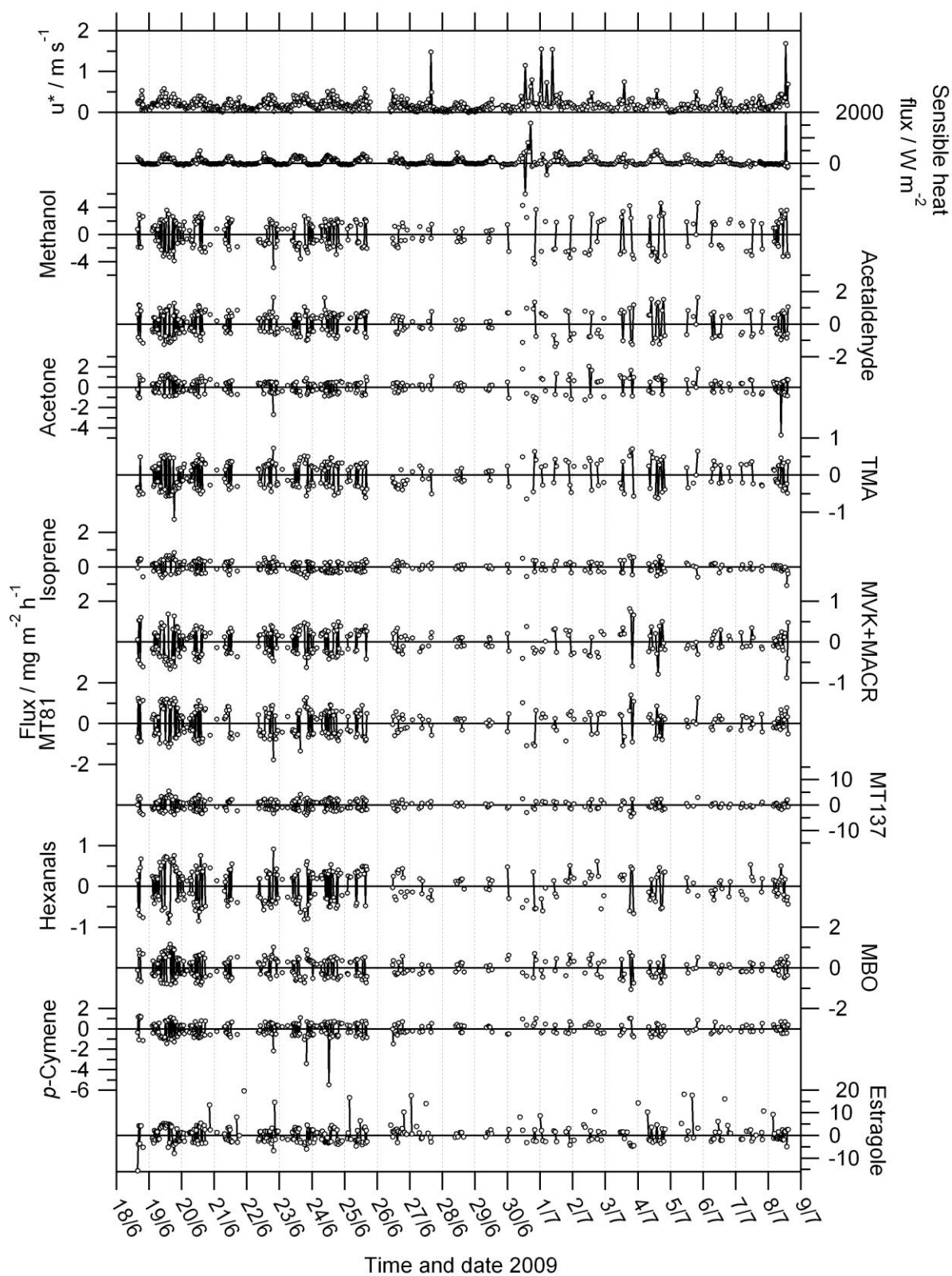
Figure S6: Average diurnal profiles of VOC fluxes above Douglas fir and of sensible heat flux, after 20:00 on 29 June 2009. Data points are the mean of median values for a ±1.5 hour time window. Note the variable scales. Grey areas show variability calculated as ±1 sd.
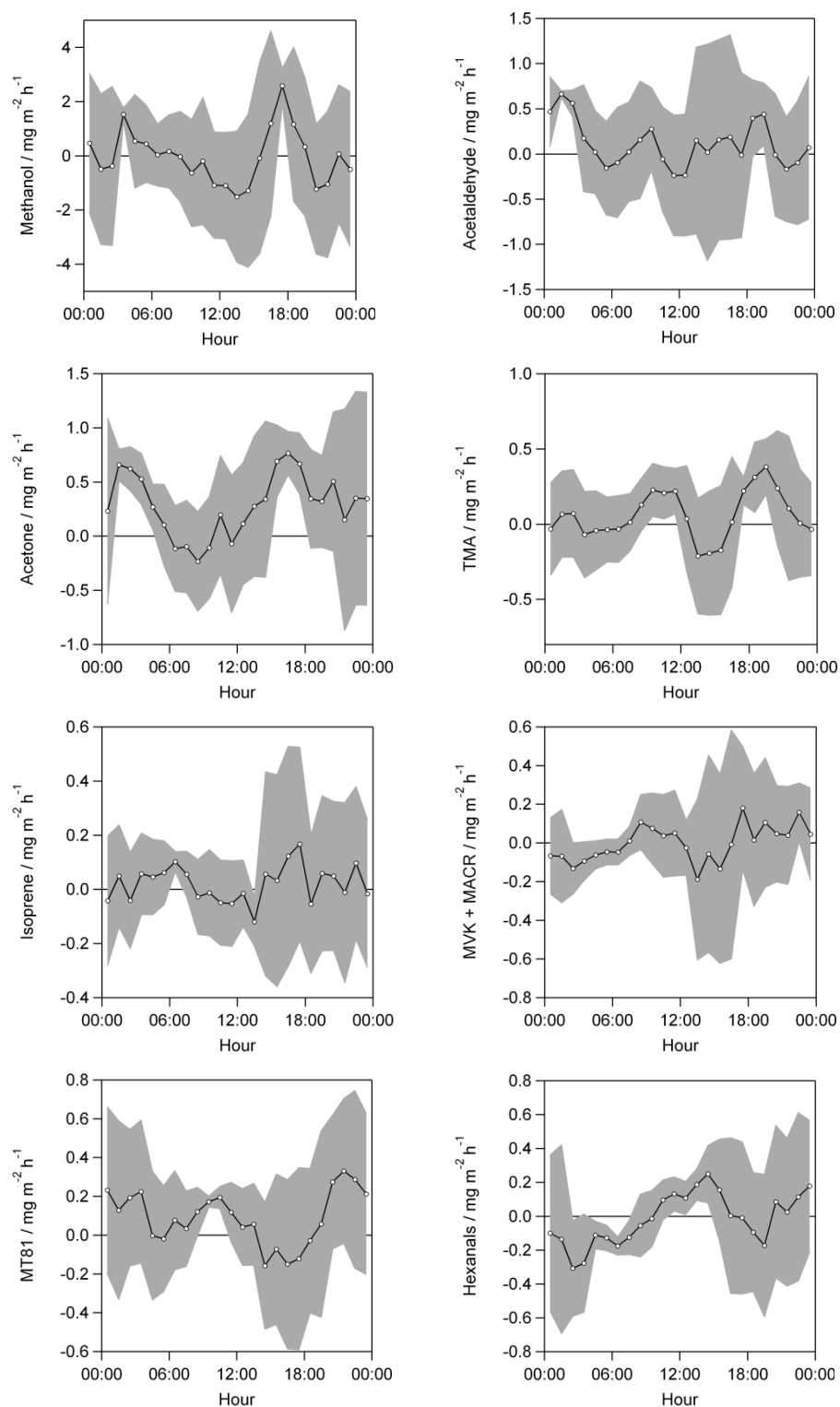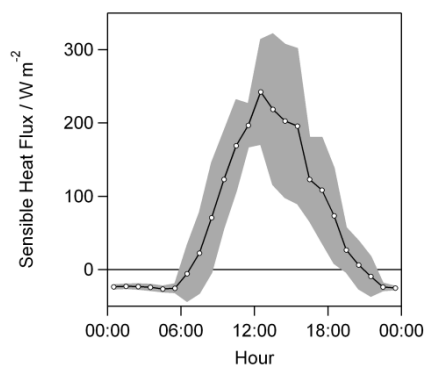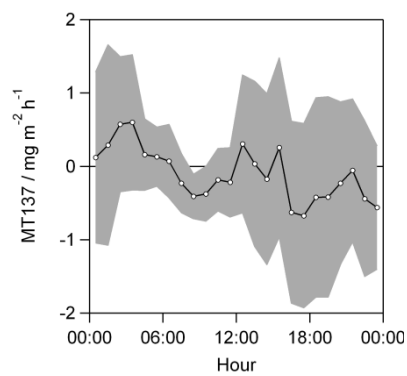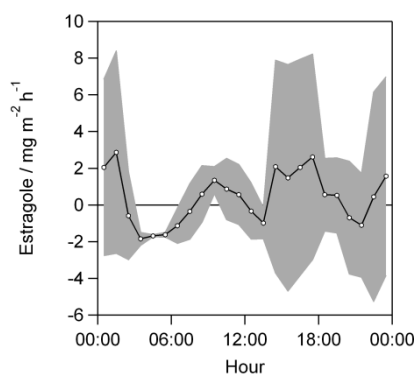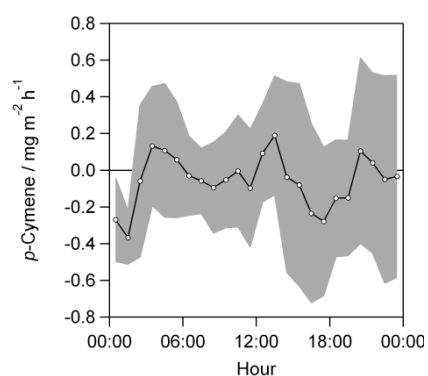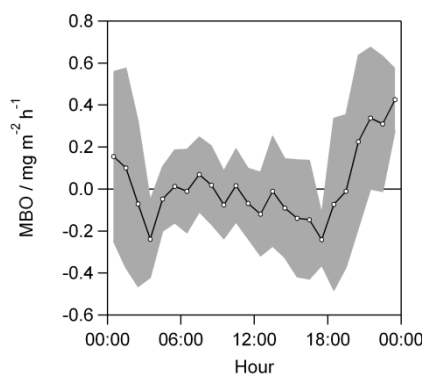
Figure S7: Time series of VOC mixing ratios, and of temperature, measured above Douglas fir. Dashed gridlines denote midnight. Note the variable mixing ratio scales.
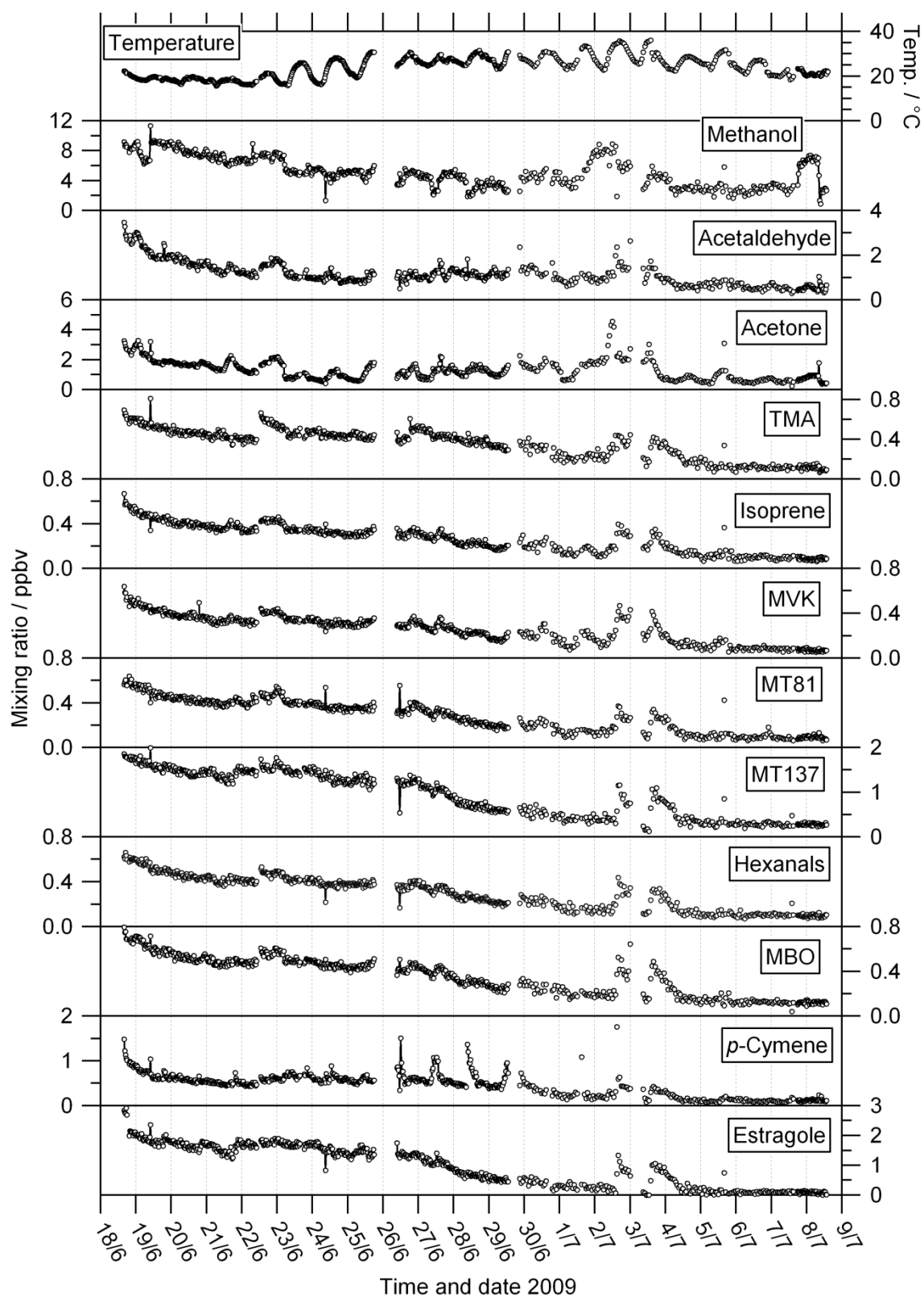
Figure S8: Average diurnal profiles of VOC mixing ratios above Douglas fir, and of temperature, after 20:00 on 29th June 2009. Note the variable scales. Dashed lines denote LOD. Grey areas show variability calculated as ±1 sd of the averaged half-hourly values of all measurements.
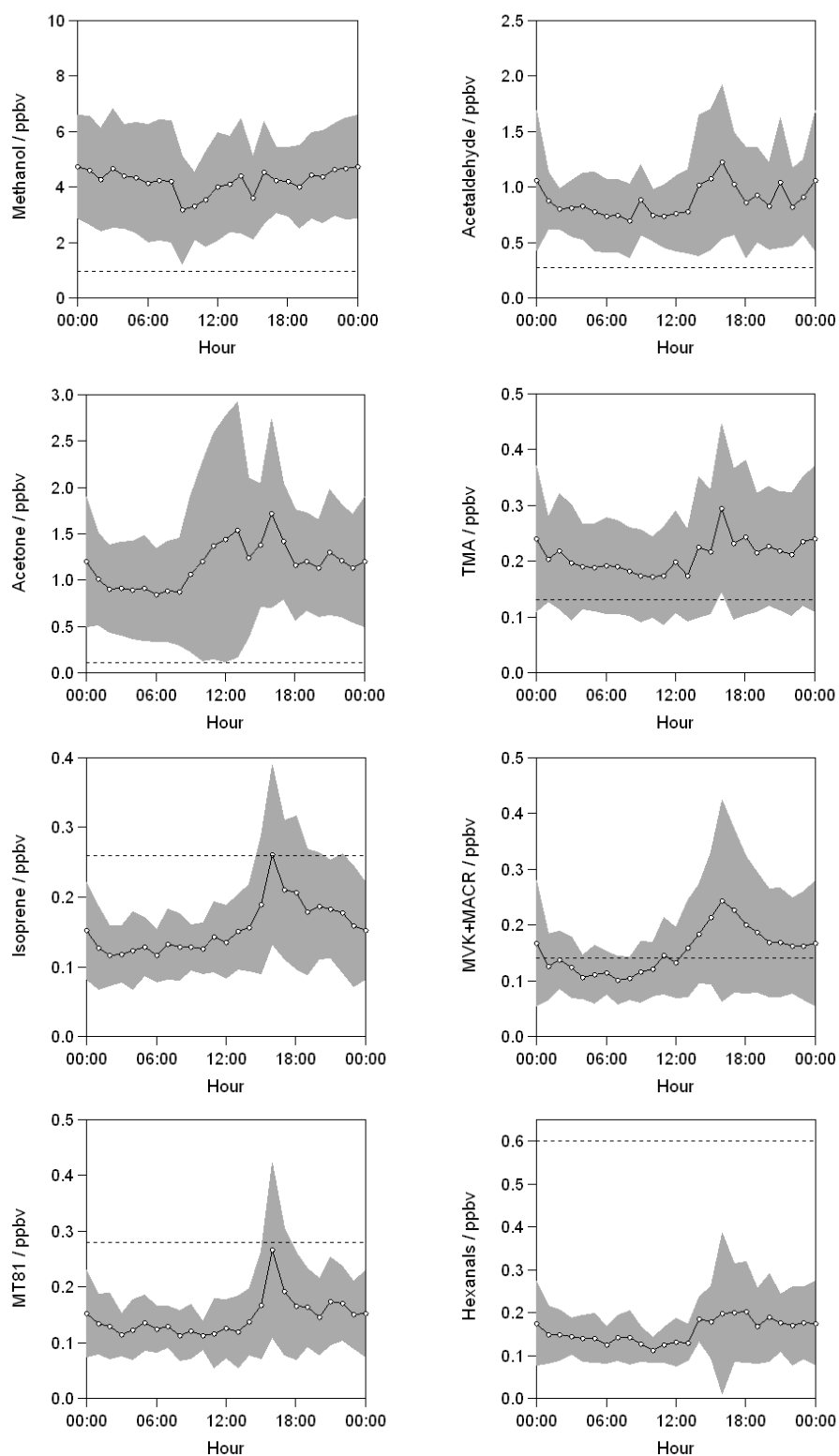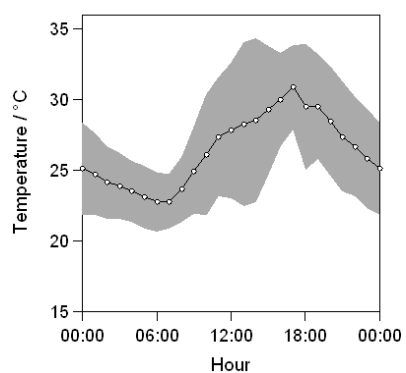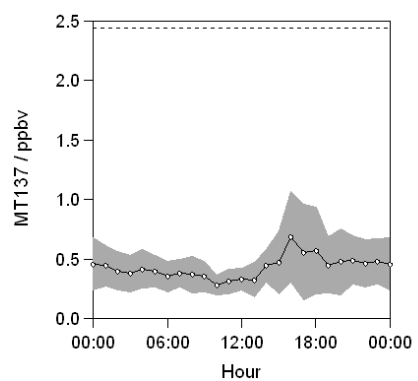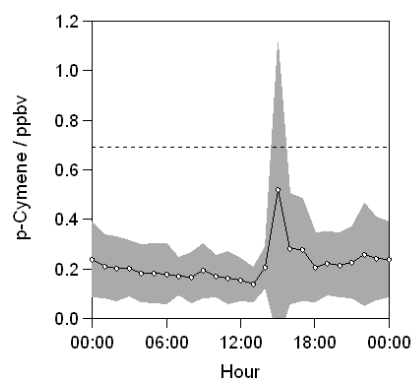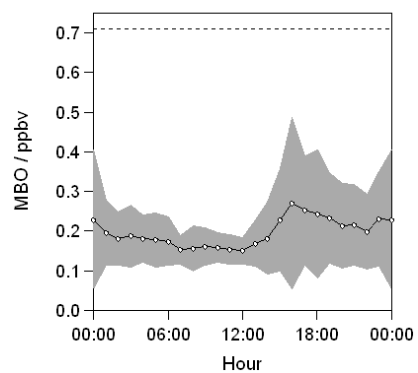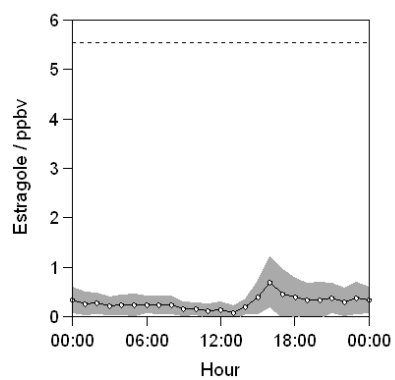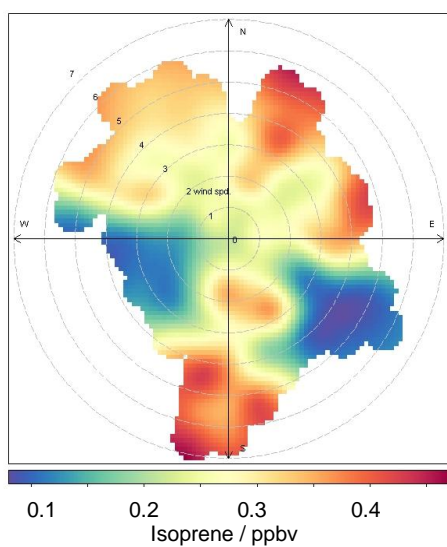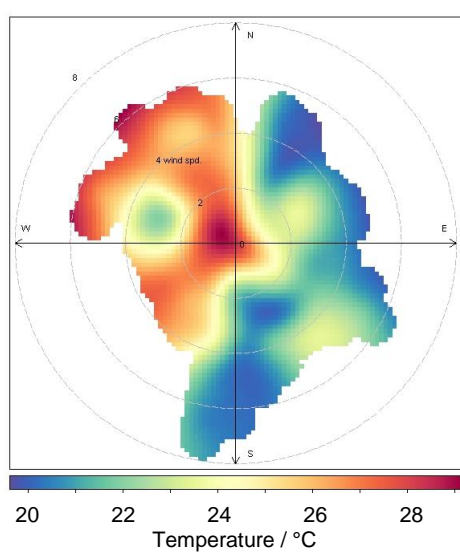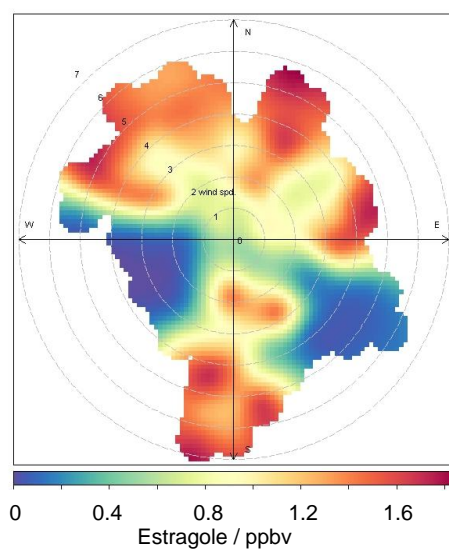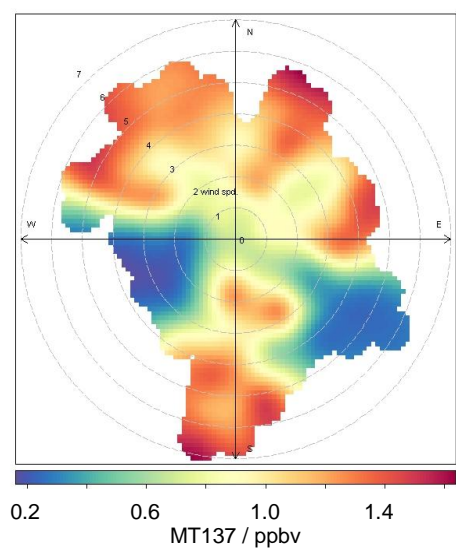
Figure S9: Bivariate plots of VOC mixing ratio by wind speed and wind direction. Polar coordinates correspond to wind direction, radial distance indicates wind speed (m s$^{-1}$) and colour denotes VOC mixing ratio according to the key for each individual plot. Temperature (°C) is shown for comparison.

Isoprene / ppbv

MVK+MACR / ppbv

MT81 / ppbv

Hexanals / ppbv

MBO / ppbv

*p*-Cymene / ppbv

13

MT137 / ppbv



Estragole / ppbv



Temperature / °C
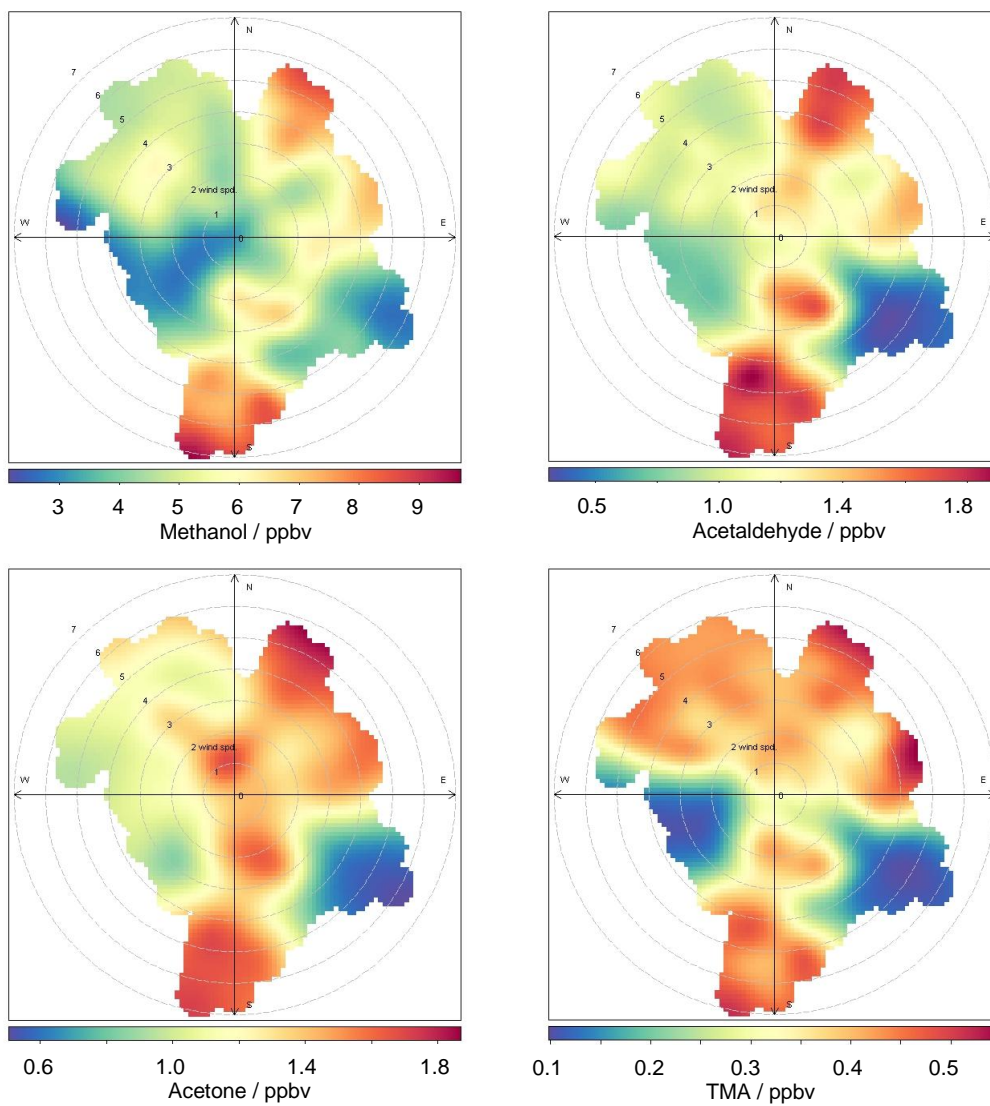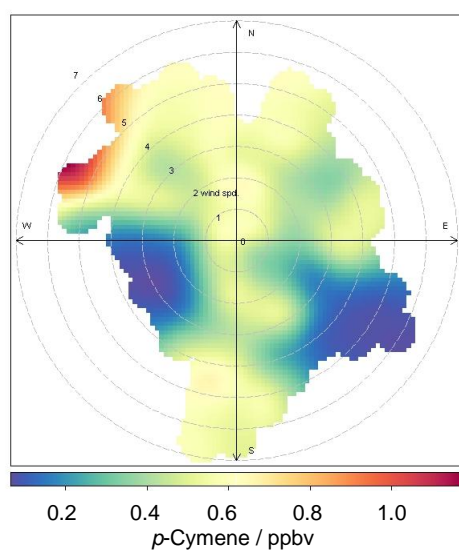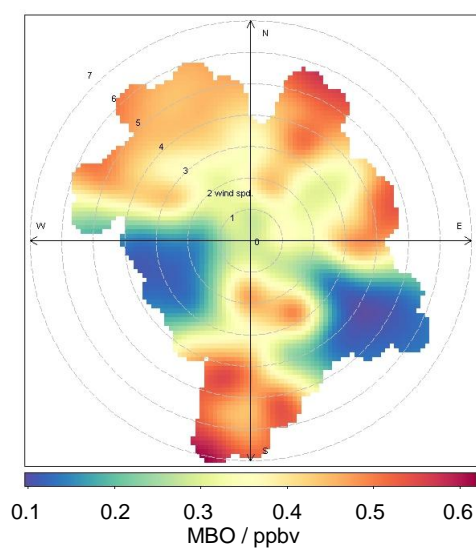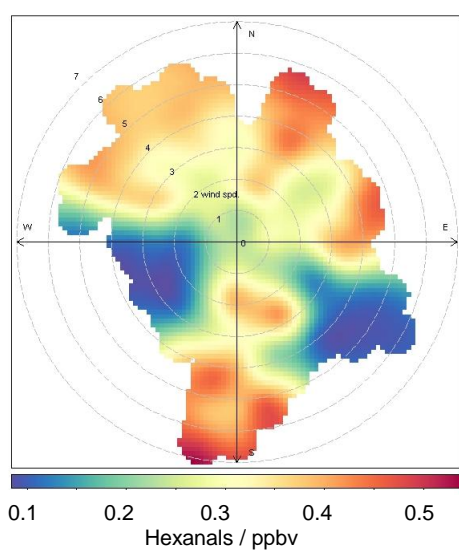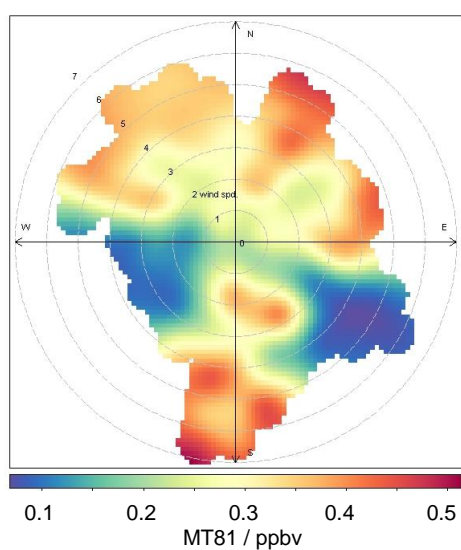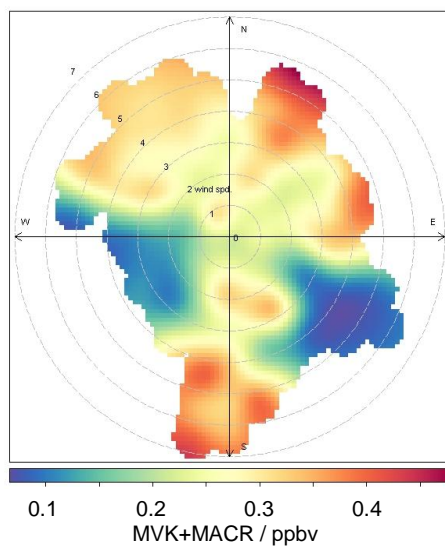
**GC-MS analyses of ambient air samples**

**Methods**

Ambient air samples were collected above the canopy (~40 m) approximately hourly from 08:10 to 20:08 on 6 July 2009 for subsequent GC-MS analysis. Samples were also taken at heights of 32, 18 and 4 m three times throughout the day (~09:30, 13:30 and 17:30) on 1 and 6 July 2009. A mass-flow controlled Pocket Pump (210-1000 Series, SKC Inc.) was used to pump air at 150 mL min$^{-1}$ for 15 min through stainless steel adsorbent tubes (6 mm OD) packed with 200 mg Tenax TA and 100 mg CarboTrap (Markes International Ltd., UK). Prior to sampling, packed tubes had been conditioned at 300 °C for 15 min in a flow of He.

Analyses were undertaken using a Hewlett-Packard 5890/5970 GC-MS with an automated thermal desorption unit (ATD 400, Perkin Elmer) connected via a 200 °C heated transfer line. Transfer of samples from adsorbent tubes was performed in two steps: heat to 280 °C for 5 min at 25 mL min$^{-1}$ to desorb samples onto a Tenax-TA cold trap at −30 °C, followed by transfer to the GC column at 300 °C for 6 min. Chromatographic separation utilised an Ultra-2 column (Agilent Technologies, 50 m × 0.2 mm ID × 0.11 µm film, 5% phenylmethyl silica) and temperature program of 35 °C for 2 min, heat at 5 °C min$^{-1}$ to 160 °C, heat at 10 °C min$^{-1}$ to 280 °C, and hold for 5 min.

A mixed monoterpene in methanol standard was prepared for calibration (10 ng µL$^{-1}$ α-pinene, β-pinene, α-phellandrene, 3-carene and limonene (Sigma Aldrich, UK)). Aliquots of the standard (0, 1, 3 and 5 µL) were injected onto 4 adsorbent tubes with He carrier gas. Tubes continued to be purged with He for 2 min after injection. LODs for α-pinene and limonene were 0.23 and 0.30 ng on column, corresponding to mixing ratios of 18 and 24 pptv, respectively, for a 2.25 L sample. The GC-MS was subject to regular calibration: a set of standards was inserted between every 8 samples. Any intervening drift was accounted for. In addition, an extensive cross-check of PTR-MS and GC-MS calibration was carried out around this time, as described in the supplementary material of Misztal et al. (2011).

No in-line ozone scrubber was used, so it is acknowledged that there may have been uncharacterised losses of the reactive VOC from oxidation by ozone during the sampling and/or other on-tube interactions/rearrangements (Larsen et al., 1997; Helmig, 1997; Pollmann et al., 2005). The co-current collection of these samples (which occurred on 2 days out of the 4 week campaign) was only for the purposes of a spot inter-comparison against the continuous

PTR-MS data, and to provide an indication of speciation between α-pinene and β-pinene, which the PTR-MS cannot distinguish.

The rate coefficients between $O_3$ and the four terpenes determined by GC-MS – α-pinene, β-pinene, 3-carene and limonene – are, respectively, 9.4, 1.9, 4.8 and 21 × 10$^{-17}$ cm$^3$ molecule$^{-1}$ s$^{-1}$ at 298 K (http://iupac.pole-ether.fr). Based on simple first-order kinetics it is possible that during 1 h of sampling up to ~25% of α-pinene could be lost by reaction but only ~5% β-pinene. This yields an effective potential bias of ~20-25% in the GC-MS determination the α-pinene:β-pinene ratio, i.e. the GC-MS data underestimate this ratio. Limonene is a factor of two more reactive to $O_3$ than the other three detected terpenes; consequently the true relative proportion of limonene with respect to the pinenes may be underestimated. However, the relative trends diurnally and with height through the canopy for a given terpene should still be generally represented by the GC-MS data even if the absolute concentrations are in error.

**Results and discussion**

The above-canopy monoterpene mixing ratios determined by adsorption tube sampling and GC-MS analysis on one day are shown in Figure S10. Given the uncertainties in the GC-MS values, there is general consistency in the daily pattern and magnitude of mixing ratios for the pinenes between these measurements and those determined by PTR-MS (Figures 2 and S8). Mixing ratios for all monoterpenes in Figure S10 decreased during the morning, and were not detected between 13:00 and 18:00, but increased again in the early evening. α-Pinene had the highest mixing ratio throughout the day, followed by 3-carene and β-pinene. Since α-pinene may also have been subject to the greatest sampling loss of these three terpenes it is clear that α-pinene is the dominant of these three. Limonene was detectable in small amount only at 09:00, although it is potentially subject to the greatest negative bias in sampling.

The average within-canopy total monoterpene mixing ratios determined by GC-MS are presented in Figure S11. These values compare fairly well with the in-canopy PTR-MS data (Figure 3). In-canopy (4 and 18 m) mixing ratios are highest in the morning and evening, and lowest in the afternoon, as was measured by PTR-MS. Conversely, peak mixing ratios measured in the afternoon were greater at the top of the canopy (32 m) and above (40 m). In general mixing ratios were larger at lower heights, again consistent with PTR-MS results.

The composition of total monoterpenes as a function of height through the canopy is illustrated in Figure S12. The data presented here are potentially subject to bias caused by the differntial losses of terpenes in sampling, as described above. α-Pinene is the dominant monoterpene at all heights (and its proportion may be underestimated relative to those of β-pinene and 3-carene) but its proportion of total monoterpenes decreases with height to a minimum at the canopy top (32 m) before increasing again above the canopy. The opposite vertical profile in contribution to total monoterpenes was observed for 3-carene whose contribution increased up to 32 m and decreased above canopy. The proportion of β-pinene decreased with height. Limonene made the lowest contribution to total monoterpenes with increasing contribution with canopy height (although its measurement is potentially subject to more negative bias than the other three terpenes). These results are consistent with a previous study at the Speuld site (Peters et al., 1994), and with another study which reported that α-pinene, β-pinene and 3-carene account for 95% monoterpene emissions from Douglas fir (Lerdau et al., 1995). This is reflected in Figure S12, except for measurements above the canopy (40 m) which may have been influenced by sources from the wider area.

Figure S10: Diurnal variation in monoterpene mixing ratios above the Douglas fir canopy (40 m). Samples were collected using adsorption tubes on 6 July 2009.
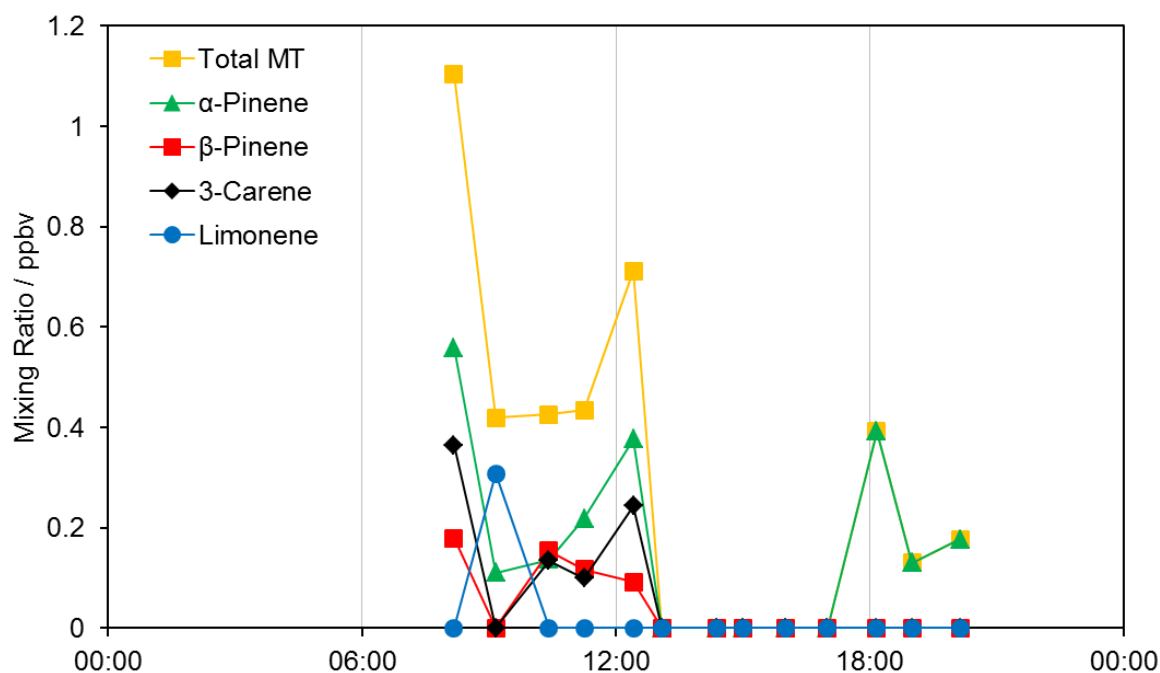
Figure S11: Average total monoterpene mixing ratios determined by GC-MS within the Douglas fir canopy. Samples were taken at three heights (4, 18 and 32 m) and at three times during the day (morning, afternoon, evening). Results shown are the averages of two sampling days (1 and 6 July) except for 40 m samples which were only taken on 6 July 2009.
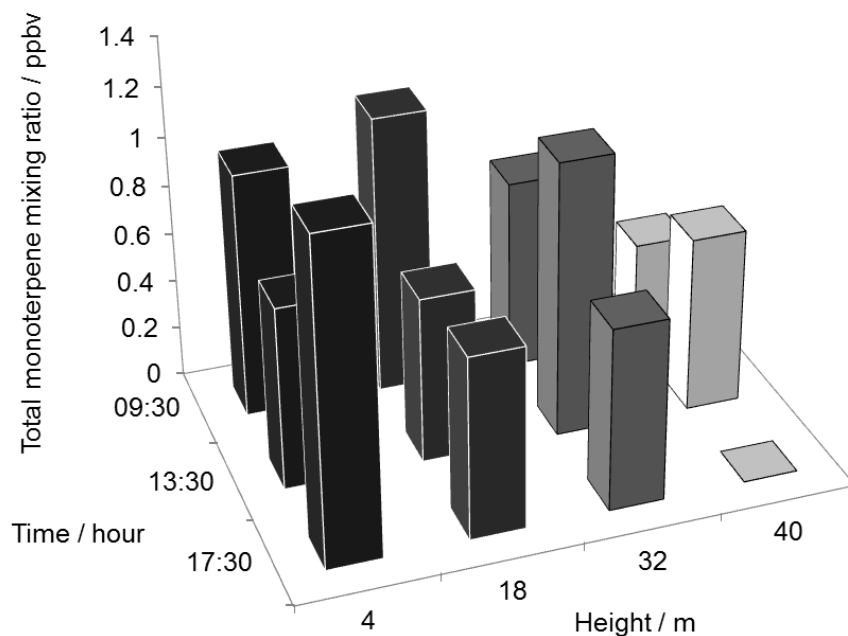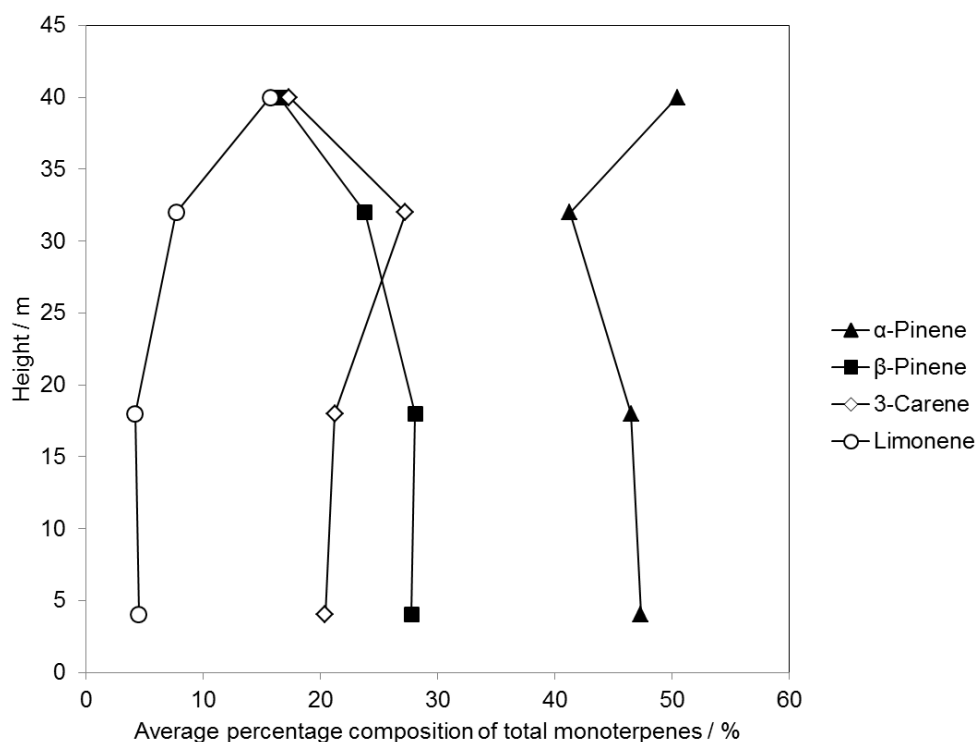


Figure S12: Monoterpene composition as a function of height above ground in the Douglas fir canopy. Each data point is a mean of 6 repeat measurements. Canopy top is at 32 m.

# References

Atkinson, R., Arey, J., 2003. Gas-phase tropospheric chemistry of biogenic volatile organic compounds: a review. Atmospheric Environment 37, S197-S219.

Bouvier-Brown, N. C., Goldstein, A. H., Worton, D. R., Matross, D. M., Gilman, J. B., Kuster, W. C., Welsh-Bon, D., Warneke, C., de Gouw, J. A., Cahill, T. M., Holzinger, R., 2009. Methyl chavicol: characterization of its biogenic emission rate, abundance, and oxidation products in the atmosphere. Atmospheric Chemistry and Physics 9, 2061-2074.

Clevers, J., Schaepman, M., Mucher, C., De Wit, A., Zurita-Milla, R., Bartholomeus, H., 2007. Using MERIS on Envisat for land cover mapping in the Netherlands. International Journal of Remote Sensing 28, 637-652.

Corchnoy, S. B., Atkinson, R., 1990. Kinetics of the Gas-Phase Reactions of OH and NO3 Radicals with 2-Carene, 1,8-Cineole, Para-Cymene, and Terpinolene. Environmental Science & Technology 24, 1497-1502.

Harrison, R. M., Hester, R. E.,  1995. *Volatile organic compounds in the atmosphere*, RSC, Cambridge.

Helmig, D., 1997. Ozone removal techniques in the sampling of atmospheric volatile organic trace gases. Atmospheric Environment 31, 3635-3651.

Jiménez, E., Lanza, B., Martinez, E., Albaladejo, J., 2007. Daytime tropospheric loss of hexanal and trans-2-hexenal: OH kinetics and UV photolysis. Atmospheric Chemistry and Physics 7, 1565-1574.

Larsen, B., Bomboi-Mingarro, T., Brancaleoni, E., et al , 1997. Sampling and analysis of terpenes in air. An interlaboratory comparison. Atmospheric Environment 31, 35-49.

Lee, D., Wexler, A. S., 2013. Atmospheric amines – Part III: Photochemistry and toxicity. Atmospheric Environment 71, 95-103.

Lerdau, M., Matson, P., Fall, R., Monson, R., 1995. Ecological Controls Over Monoterpene Emissions from Douglas-Fir (*Pseudotsuga-Menziesii*). Ecology 76, 2640-2647.

Misztal, P. K., Nemitz, E., Langford, B., Di Marco, C. F., Phillips, G. J., Hewitt, C. N., MacKenzie, A. R., Owen, S. M., Fowler, D., Heal, M. R., Cape, J. N., 2011. Direct ecosystem fluxes of volatile organic compounds from oil palms in South-East Asia. Atmospheric Chemistry and Physics 11, 8995-9017.

Peters, R. J. B., Duivenbode, J. A. D. V., Duyzer, J. H., Verhagen, H. L. M., 1994. The determination of terpenes in foreset air. Atmospheric Environment 28, 2413-2419.

Pollmann, J., Ortega, J., Helmig, D., 2005. Analysis of atmospheric sesquiterpenes: Sampling losses and mitigation of ozone interferences. Environmental Science & Technology 39, 9620-9629.

Schade, G. W., Goldstein, A. H., 2001. Fluxes of oxygenated volatile organic compounds from a ponderosa pine plantation. Journal of Geophysical Research-Atmospheres 106, 3111-3123.